

Articles

Helix-Sense-Controlled Polymerization of Optically Active Phenyl Isocyanides

Takashi Kajitani,[†] Kento Okoshi,^{*,†} and Eiji Yashima^{*,†,‡}

Yashima Super-structured Helix Project, Exploratory Research for Advanced Technology (ERATO), Japan Science and Technology Agency (JST), 101 Creation Core Nagoya, 2266-22 Anagahora, Shimoshidami, Moriyama-ku, Nagoya 463-0003, Japan, and Graduate School of Engineering, Nagoya University, Nagoya 464-8603, Japan

Received October 16, 2007; Revised Manuscript Received December 26, 2007

ABSTRACT: A series of optically active phenyl isocyanides bearing various chiral functional groups, such as L-alanine, L-alaninol, L-phenylalanine, and L-lactic acid residues, with a long *n*-decyl chain as the pendants were prepared, and these were polymerized with an achiral nickel catalyst (NiCl₂) in various organic solvents at different temperatures. The chiroptical properties and structures of the resulting helical polyisocyanides investigated by circular dichroism (CD) and IR spectroscopy revealed that the Cotton effect signs and intensities of the polyisocyanides, which correspond to their helical senses (right- or left-handed helix) and the excess of one helical sense, respectively, were significantly dependent on the pendant structures of the polymers and the polymerization conditions, such as the solvent polarity and temperature. The effect of the alkyl chain length of L-alanine-bound phenyl isocyanides on the helix-sense-controlled polymerization was also investigated.

Introduction

The synthesis of optically active polymers with a single-handed helical conformation has attracted much attention not only to mimic biological helical structures but also for their prospective applications to chiral materials, such as liquid crystals¹ and enantioselective adsorbents.² To this end, optically active helical polymers have been prepared either by the polymerization of specific nonracemic monomers or by the helix-sense-selective polymerization of achiral or prochiral bulky monomers with chiral catalysts or initiators.^{2d,3}

Polyisocyanides are among the most extensively studied helical polymers since the pioneering research by Millich, Drenth, and Nolte.^{3b,4} The helical structure of polyisocyanides has been considered to be stable with a 4 units/turn (4/1) helix when they have a bulky side group^{3b,4a–d,5} as evidenced by the direct chromatographic resolution of poly(*tert*-butyl isocyanide) into enantiomeric helices⁶ and further proved by the helix-sense-selective polymerization of achiral bulky isocyanides by Nolte⁷ and Novak.⁸ Since then, wide varieties of helical polyisocyanides with functional pendant groups have been prepared, and some of them were utilized for optoelectronic and liquid crystalline materials.^{3b,4d,g,9} Nolte and co-workers also developed a series of helical poly(isocyanopeptide)s bearing amino acid or peptide residues as the pendant groups stabilized by intramolecular hydrogen bonds in which their helical senses are determined by the amino acid chirality of the pendants.^{1d,e,j,3b,4d,m,r,5d,9b}

Recently, we reported an unprecedented helix-sense-controlled polymerization of enantiomerically pure phenyl isocya-

nides bearing an L- or D-alanine pendant with a long *n*-decyl chain (**3** in Scheme 1). In sharp contrast to the poly(isocyanopeptide)s, the polymerization with an achiral nickel catalyst (NiCl₂) diastereoselectively proceeded, resulting in an either right- or left-handed helical polymer (poly-**3**), whose helical sense can be controlled by the polymerization solvent and temperature.¹⁰ An intermolecular hydrogen bond between the pendant amide residues of the growing chain end and **3** during the propagation reaction appeared to play a crucial role for the polyisocyanide to form either kinetically or thermodynamically stable right- or left-handed helical structure.

In this study, we synthesized a series of optically active phenyl isocyanides bearing various chiral functional groups, such as L-alanine (**3**), L-alaninol (**5**), L-phenylalanine (**6**), and L-lactic acid residues (**7**) with a long *n*-decyl chain as the pendants, and these were polymerized with an achiral NiCl₂ catalyst in various solvents at different temperatures (Scheme 1). Analogous L-alanine-bound helical polyisocyanides with different alkyl chains (*m* = 2, 6, and 14 in Scheme 1) were also prepared by the polymerization of the corresponding monomers (**1**, **2**, and **4**). The effects of the alkyl chain length, bulkiness, and hydrogen-bonding ability of the pendant groups of these isocyanides (**1–7**) on the helix-sense-controlled polymerization and the chiroptical properties of the resulting polyisocyanides were investigated by absorption, circular dichroism (CD), and IR spectroscopies.

Results and Discussion

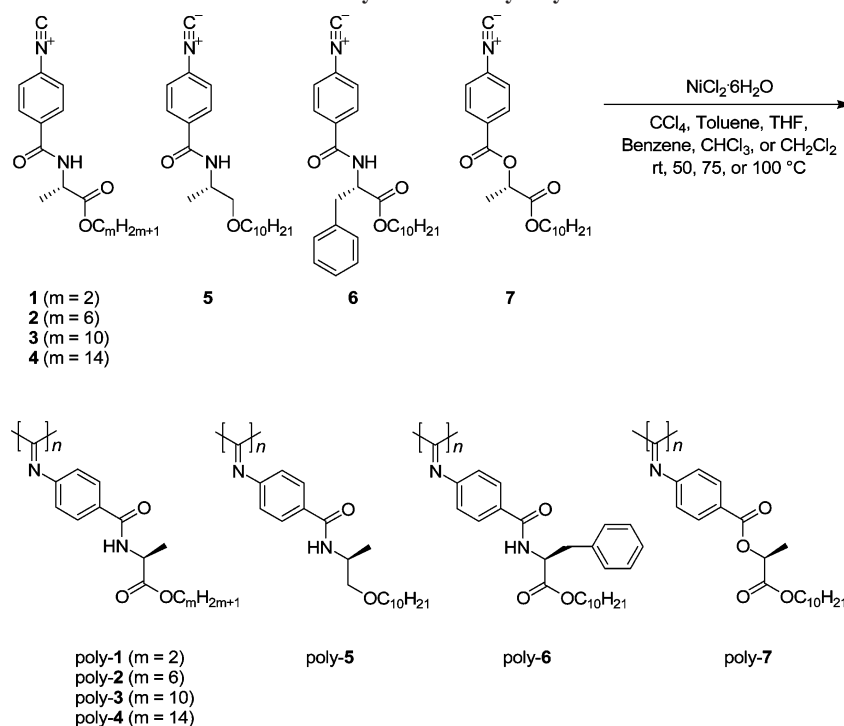
Synthesis and Polymerization of Optically Active Isocyanides. Six optically active isocyanides bearing different L-amino acid residues with a short ethyl (**1**) or long *n*-hexyl (**2**), *n*-decyl (**3**, **5**, and **6**), or *n*-tetradecyl (**4**) chain as the pendant through

* Corresponding authors. E-mail: kokoshi@yp-jst.jp; yashima@apchem.nagoya-u.ac.jp.

[†] Japan Science and Technology Agency.

[‡] Nagoya University.

Scheme 1. Synthesis of Polyisocyanides



an amide linkage (**1–6**) and an L-lactic acid-bound isocyanide with an *n*-decyl chain as the pendant through an ester linkage (**7**) were synthesized as outlined in Schemes 2 and 3 (see Experimental Section), respectively, and these were then polymerized with an achiral NiCl_2 catalyst in various organic solvents, such as nonpolar (CCl_4 and toluene) and polar (tetrahydrofuran (THF)) solvents at different temperatures (Scheme 1). The polymerization results of **1–7** are summarized in Table 1. All the polymerization reactions proceeded homogeneously and afforded high molecular weight polymers (poly-**1**–poly-**7**) in high yield (64–92%), except for poly-**4a** obtained in CCl_4 at room temperature (43% yield). The polymerization in THF at room temperature (poly-**1c**–poly-**7c**) and toluene at 100 °C (poly-**1d**–poly-**7d**) tended to give relatively higher molecular weight polymers ($M_n = (15\text{--}50) \times 10^4$) with wider polydispersity (M_w/M_n) than those polymerized in CCl_4 (poly-**1a**–poly-**7a**) and toluene (poly-**1b**–poly-**7b**) at room temperature (see Table 1). In fact, the molecular weight of poly-**3** obtained in toluene increased with an increase in the polymerization temperature (runs 10 and 12–14 in Table 1). Polymerization in benzene, CHCl_3 , and CH_2Cl_2 at room temperature was also performed for **3** to investigate the solvent effect, giving high molecular weight polymers (poly-**3g**–poly-**3i**) in high yield (runs 15–17 in Table 1).

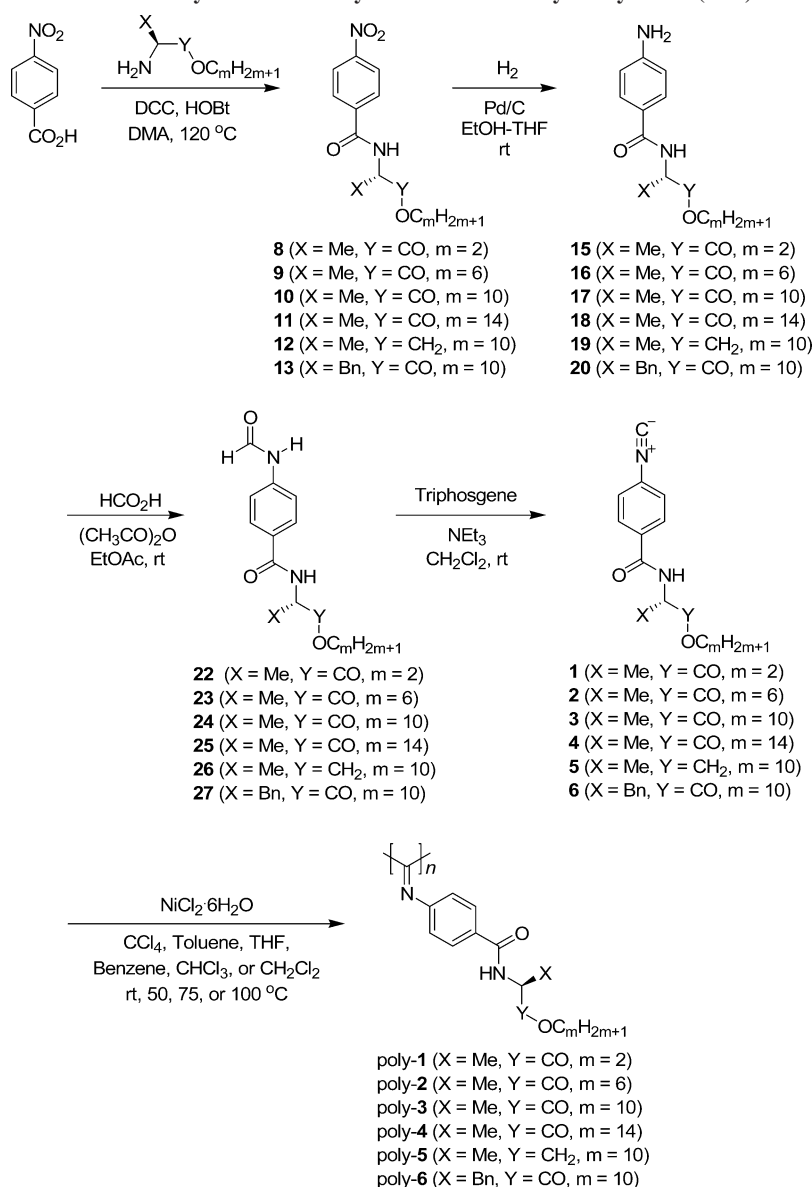
Effects of Solvent and Temperature on Helix-Sense-Controlled Polymerization of 3. First, we investigated the effects of solvent and temperature during the polymerization of **3** on the chiroptical properties of the resulting polyisocyanides. Figure 1A shows the CD spectra of poly-**3s** polymerized in various solvents at room temperature together with the typical absorption spectrum (poly-**3a**) measured in CHCl_3 at 25 °C. The sign and intensity of the first Cotton effect at around 360 nm ($\Delta\epsilon_{1st}$), which reflect the helical sense (right- or left-handed helix) and the excess of one helical sense of the polymer backbone, respectively, were significantly dependent on the polymerization solvent and temperature. The Cotton effect signs of polyisocyanides obtained by the polymerization at room

temperature in nonpolar solvents, such as CCl_4 (poly-**3a**), toluene (poly-**3b**), and benzene (poly-**3g**), were opposite to that in polar THF (poly-**3c**), suggesting that the helical senses of poly-**3a** and poly-**3c** are opposite to each other, regardless of the fact that the polymers have the same L-alanine pendants.¹¹ Poly-**3h** and poly-**3i** obtained by the polymerization in less polar CHCl_3 and CH_2Cl_2 at room temperature, respectively, also exhibited a weak, but positive $\Delta\epsilon_{1st}$ value like those in nonpolar CCl_4 and toluene (Figure 1A and runs 16 and 17 in Table 1).

We presume that the observed unusual changes in the first Cotton effect sign of the poly-**3s**, that is their helical sense, depending on the polymerization solvent may be ascribed to the “on–off” fashion of the intermolecular hydrogen bonds between the pendant amide residues of the growing chain end and **3** during the propagation reaction, which may force the poly-**3** into either a right- or left-handed helix in nonpolar solvents under predominantly kinetic control (positive $\Delta\epsilon_{1st}$ value). In polar solvents such as THF, however, such hydrogen bonding will be hampered, resulting in a thermodynamically favorable helical conformation (negative $\Delta\epsilon_{1st}$ value).¹² This speculation was supported by the NMR and IR spectra of **3** measured in polar and nonpolar solvents.¹³ The amide NH protons of **3** were largely shifted downfield in THF- d_8 (7.98 ppm) due to strong solvation compared with those in CD_2Cl_2 (6.82 ppm) and toluene- d_8 (6.61 ppm) (Figures S1 and S3A). The NH and amide II bands of **3** in THF significantly shifted to shorter and longer wavenumbers, respectively (Figures S2 and S3B); the band positions also suggest solvated NH residues of **3** by THF molecules. In addition, the fact that polymerization of an analogous isocyanide in which the amide linkage was replaced by an ester one (**7**) produced a helical polyisocyanide with the same handedness independent of the polymerization conditions also supports our speculation (see below and Figure 4C).

We then polymerized **3** in nonpolar toluene at high temperatures (50, 75, and 100 °C) with the expectation that helical polyisocyanides with the same handedness as that of the poly-

Scheme 2. Synthesis and Polymerization of Phenyl Isocyanides (1–6)



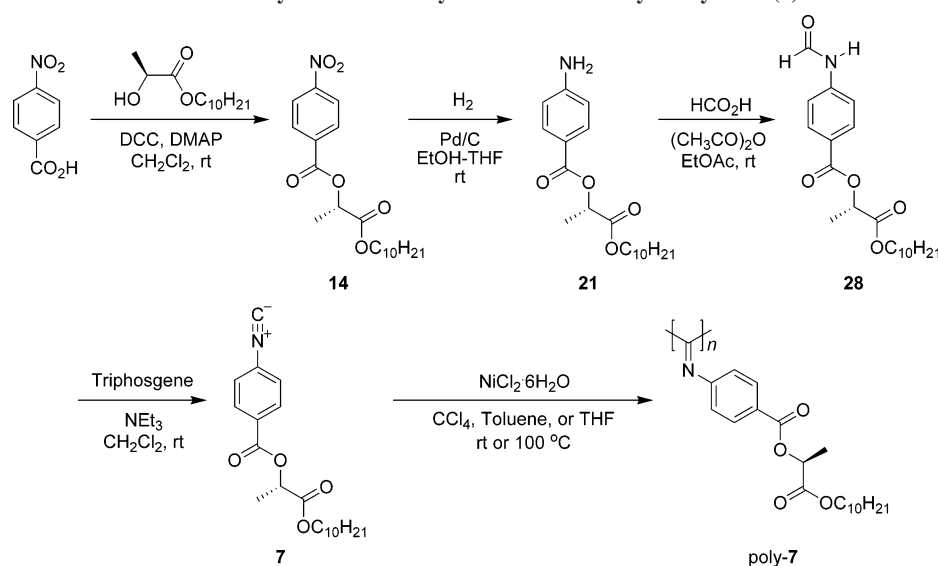
3c would be produced (Figure 1B). In fact, poly-**3** obtained by the polymerization of **3** in toluene at 75 °C (poly-**3f**) exhibited the opposite negative $\Delta\epsilon_{1st}$ value (−2.47) to that of poly-**3b** (+2.25), and the CD intensity further increased in the negative direction when polymerized in toluene at 100 °C (poly-**3d**, $\Delta\epsilon_{1st}$ = −4.64). The specific rotation ($[\alpha]_D^{25}$) also changed from +98.5° (poly-**3b**) to −410° (poly-**3d**, see Table 1 and Figure S4). We note that the IR spectra of poly-**3s** clearly evidenced the formation of intramolecular hydrogen bonds regardless of the polymerization conditions, indicating that both the right- and left-handed helices are stabilized more or less by intramolecular hydrogen bonds after the polymerization (see Table S1 and below for more detailed discussion).

Effect of Alkyl Chain Length of L-Alanine-Bound Isocyanides (1–4) on Helix-Sense-Controlled Polymerization. Next, we investigated the effect of the alkyl chain length of the pendant groups of L-alanine-bound isocyanides (**1–4**) on the helix-sense-controlled polymerization and the chiroptical properties of the polymers. L-Alanine-bound helical polyisocyanides with different *n*-alkyl chains (*m* = 2, 6, and 14 in Scheme 1) were prepared in the same way by the polymerization of the corresponding monomers (**1**, **2**, and **4**) with NiCl₂ catalyst in

nonpolar (CCl₄ and toluene) and polar (THF) solvents at room temperature and in toluene at 100 °C (Table 1).

The CD spectra of a series of polyisocyanides (poly-**1**–poly-**4**) are shown in Figure S5, and the relationships between the pendant alkyl chain length (*m*) of the polymers and their $\Delta\epsilon_{1st}$ values are depicted in Figure 2. The polymers prepared in nonpolar solvents (CCl₄ and toluene) at room temperature and in toluene at 100 °C exhibited the same positive and negative Cotton effect signs, respectively, independent of the chain length (*m*), although the CD intensities are different from each other. Notably, poly-**1d** showed a very intense negative $\Delta\epsilon_{1st}$ value (−12.6) (run 4 in Table 1). However, the Cotton effect signs of the polymers prepared in polar THF at room temperature were considerably affected by the alkyl chain length; the poly-**1c** and poly-**2c** with a short ethyl and *n*-hexyl chain, respectively, exhibited the same positive Cotton effect sign as those of poly-**1**–poly-**4** prepared in nonpolar solvents at room temperature, while the poly-**3c** and poly-**4c** with a long *n*-decyl and *n*-tetradecyl chain, respectively, showed the opposite negative $\Delta\epsilon_{1st}$ value as described above. Although it still remains unclear why the sign of the Cotton effects of the poly-**1c** and poly-**2c** was reversed among the L-alanine-bound polyisocyanides, the

Scheme 3. Synthesis and Polymerization of Phenyl Isocyanide (7)

Table 1. Polymerization Results of Phenyl Isocyanides with $\text{NiCl}_2 \cdot 6\text{H}_2\text{O}^a$

run	polymer	polymerization conditions		yield (%)	$M_n \times 10^{-4}{}^b$	$M_w/M_n{}^b$	$[\alpha]_{\text{D}}^{25}{}^c$	$\Delta\epsilon_{\text{1st}}{}^c$
		solvent	temp					
1	poly-1a	CCl_4	rt	90.3	3.7	1.9	+680	+6.97
2	poly-1b	toluene	rt	80.3	4.5	1.9	+377	+3.70
3	poly-1c	THF	rt	86.8	47	2.6	+247	+3.45
4	poly-1d	toluene	100 °C	72.4	50	3.1	−1180	−12.6
5	poly-2a	CCl_4	rt	82.7	12	1.4	+1020	+9.90
6	poly-2b	toluene	rt	75.2	16	1.3	+146	+2.64
7	poly-2c	THF	rt	80.1	43	1.5	+55.3	+0.32
8	poly-2d	toluene	100 °C	85.4	41	1.8	−705	−7.26
9	poly-3a	CCl_4	rt	78.1	8.4	1.4	+616	+8.14
10	poly-3b	toluene	rt	89.2	6.7	1.8	+98.5	+2.25
11	poly-3c	THF	rt	81.7	28	2.2	−59.0	−1.28
12	poly-3d	toluene	100 °C	82.7	25	2.4	−410	−4.64
13	poly-3e	toluene	50 °C	84.6	9.3	2.1	+60.8	+0.41
14	poly-3f	toluene	75 °C	78.4	20	2.0	−137	−2.47
15	poly-3g	benzene	rt	80.4	15	1.3	+325	+5.02
16	poly-3h	CHCl_3	rt	87.6	13	1.4	+293	+2.83
17	poly-3i	CH_2Cl_2	rt	91.6	22	1.4	+56.4	+0.52
18	poly-4a	CCl_4	rt	42.8	11	1.5	+671	+8.03
19	poly-4b	toluene	rt	65.2	12	1.5	+155	+1.22
20	poly-4c	THF	rt	86.7	28	1.3	−326	−5.14
21	poly-4d	toluene	100 °C	77.1	48	1.4	−420	−6.25
22	poly-5a	CCl_4	rt	71.6	6.2	1.6	−177	−1.43
23	poly-5b	toluene	rt	63.5	7.5	1.7	−107	−0.63
24	poly-5c	THF	rt	87.0	41	2.3	−64.2	+0.42
25	poly-5d	toluene	100 °C	80.9	30	2.5	−273	−1.28
26	poly-6a	CCl_4	rt	64.2	6.5	1.3	+439	+6.99
27	poly-6b	toluene	rt	69.5	11	1.9	+390	+5.47
28	poly-6c	THF	rt	78.5	28	1.9	+364	+5.40
29	poly-6d	toluene	100 °C	80.0	26	2.4	+688	+8.94
30	poly-7a	CCl_4	rt	81.3	27	1.5	−115	−1.68
31	poly-7b	toluene	rt	76.4	8.7	1.9	−157	−1.96
32	poly-7c	THF	rt	78.2	15	2.2	−177	−2.37
33	poly-7d	toluene	100 °C	72.1	22	1.8	−243	−3.21

^a Polymerized under nitrogen; [monomer] = 0.1 M, [monomer]/[Ni] = 100. ^b Determined by SEC (polystyrene standards) with THF containing tetra-*n*-butylammonium bromide (0.1 wt %) as the eluent. ^c Measured in CHCl_3 at 25 °C.

helical senses of polyisocyanides may be determined in a delicate fashion that is balanced by solvation (intermolecular hydrogen bonding), temperature, and steric effect of the pendants during the polymerization.

Annealing Effect of Helical Polyisocyanides. We then investigated the annealing effect of L-alanine-bound helical polyisocyanides with different *n*-alkyl chains (poly-1–poly-4). As reported previously, the negative $\Delta\epsilon_{\text{1st}}$ values of poly-3c and poly-3d with a long *n*-decyl chain prepared in polar THF at room temperature and nonpolar toluene at 100 °C, respectively,

slowly but dramatically increased with time at high temperature and reached $\Delta\epsilon_{\text{1st}} = -8.5$ and -11.8 , respectively, after the polymers were annealed in toluene at 100 °C for 12 days (Figures 3A and S6, respectively).^{10,14} Under the same conditions, the poly-3a prepared in nonpolar CCl_4 at room temperature showed a decrease in the positive CD intensity of ca. 31% (Figure S6).¹⁵ Interestingly, the positive first Cotton effect signs of poly-1c and poly-2c with a short ethyl and *n*-hexyl chain, respectively, prepared in polar THF at room temperature were reversed immediately after annealing the polymers in toluene

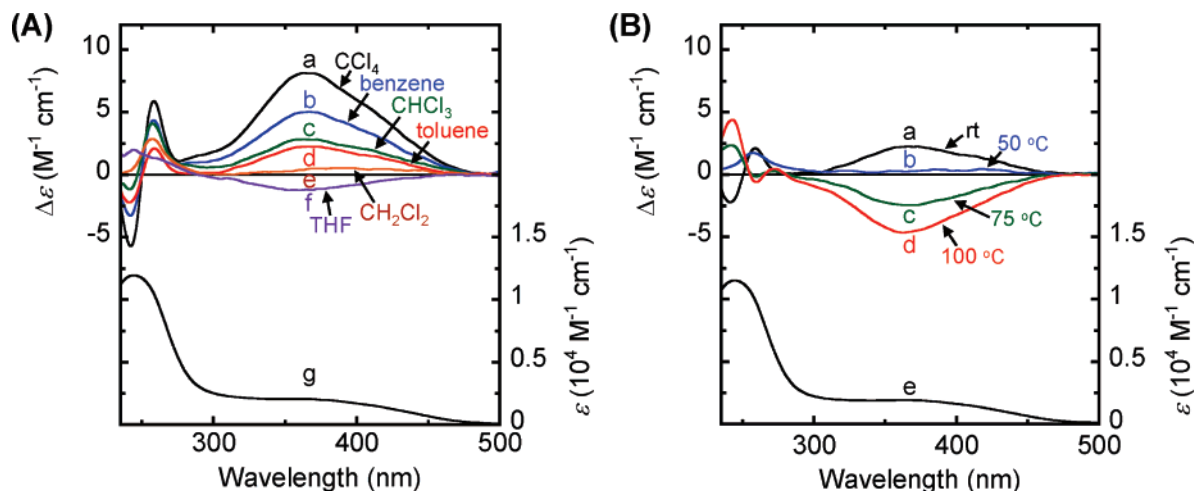


Figure 1. (A) CD spectra of poly-3a (a, black line), poly-3g (b, blue line), poly-3h (c, green line), poly-3b (d, red line), poly-3i (e, brown line), and poly-3c (f, purple line) polymerized in CCl₄, benzene, CHCl₃, toluene, CH₂Cl₂, and THF, respectively, at room temperature. The absorption spectrum of poly-3a (g) is also shown. (B) CD spectra of poly-3b (a, black line), poly-3e (b, blue line), poly-3f (c, green line), and poly-3d (d, red line) polymerized in toluene at room temperature (ca. 25 °C), 50, 75, and 100 °C, respectively. The CD and absorption spectra were measured in CHCl₃ at 25 °C (0.2 mg/mL).

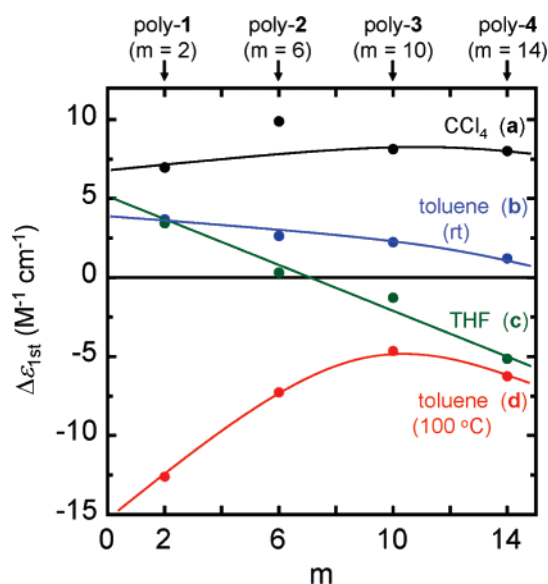


Figure 2. Relationships between the pendant alkyl chain length (m) and the first Cotton effect intensity at around 360 nm ($\Delta\epsilon_{1st}$) of poly-1–poly-4 polymerized in CCl₄ (black line), toluene (blue line), THF (green line) at room temperature, and in toluene at 100 °C (red line). The CD spectra were measured in CHCl₃ at 25 °C (0.2 mg/mL).

at 100 °C, and the negative $\Delta\epsilon_{1st}$ values gradually increased to -3.18 and -6.69 , respectively, after 12 days (Figure 3A). In addition, the CD intensity of poly-4c with a longer n -tetradecyl chain ($\Delta\epsilon_{1st} = -5.14$) further increased in the negative direction after annealing in toluene at 100 °C (Figure 3A). These results indicate that the helical conformations of the polyisocyanides prepared in THF at room temperature are not stable and changed into a thermodynamically more stable left-handed helical conformation with an excess single-handed helix upon heating. In contrast, polyisocyanides prepared in nonpolar CCl₄ at room temperature (poly-1a–poly-4a) possessed a relatively stable helical conformation generated during the polymerization under predominantly kinetic control and maintained their positive $\Delta\epsilon_{1st}$ values after annealing in toluene at 100 °C (for example, see Figure S6 (poly-3a)). The successive sequence of intramolecular hydrogen bonds between the pendant amide residues of the polymers likely contributes to maintaining their kinetically

controlled helical conformations upon heating. Therefore, the polyisocyanides prepared in toluene at 100 °C (poly-1d–poly-4d) produced helical polyisocyanides with an opposite Cotton effect sign.

Effect of Chiral Pendant Structures of Isocyanides (5–7) on Helix-Sense-Controlled Polymerization. Figure 4 shows the CD spectra of poly-5–poly-7 polymerized in nonpolar CCl₄ and toluene and polar THF at room temperature and in toluene at 100 °C (see also Table 1). Poly-5 and poly-7 in which the ester and amide linkages of poly-3 were replaced by ether and ester ones, respectively, exhibited weak negative $\Delta\epsilon_{1st}$ values independent of the polymerization conditions (Figure 4A and 4C, respectively), except for the poly-5c ($\Delta\epsilon_{1st} = +0.42$). In addition, the CD intensity of poly-7c prepared in THF at room temperature hardly changed after annealing the polymer in toluene at 100 °C for 12 days, and that of poly-5c slightly changed under the same conditions (Figure 3B). These results indicate that the amide residues as well as the ester carbonyl groups at the pendant groups play an important role in preparing helical polyisocyanides with a controlled helical sense during the polymerization.

In contrast, poly-6 bearing an *L*-phenylalanine pendant with an n -decyl chain whose structural characteristic is quite similar to that of poly-3 except for its bulkiness exhibited rather intense positive $\Delta\epsilon_{1st}$ values independent of the polymerization conditions (Figure 4B and Table 1). In other words, the right-handed helical conformation showing the positive first Cotton effect sign^{5e,10} was preferably formed during the polymerization of 6 independent of the solvent polarity and temperature, probably because of the bulky *L*-phenylalanine residue which may force the poly-6 into a right-handed helix in any solvent under predominantly kinetic control. FT-IR spectra of a series of polyisocyanides (poly-1–poly-7) taken at room temperature in dilute CHCl₃ solutions (5.0 mg/mL) and in KBr provide insight into the effect of the functional groups on the structures of the polyisocyanides prepared by the helix-sense-controlled polymerization (Table S1). Almost all the bands arising from the NH, the ester carbonyl, and the amide I for the *L*-alanine- and *L*-phenylalanine-bound polyisocyanides (poly-1–poly-4 and poly-6) appeared at around 3266–3286, 1737–1746, and 1633–1638 cm^{-1} , respectively, the positions of which prove the formation of intramolecular hydrogen bonding. However, the

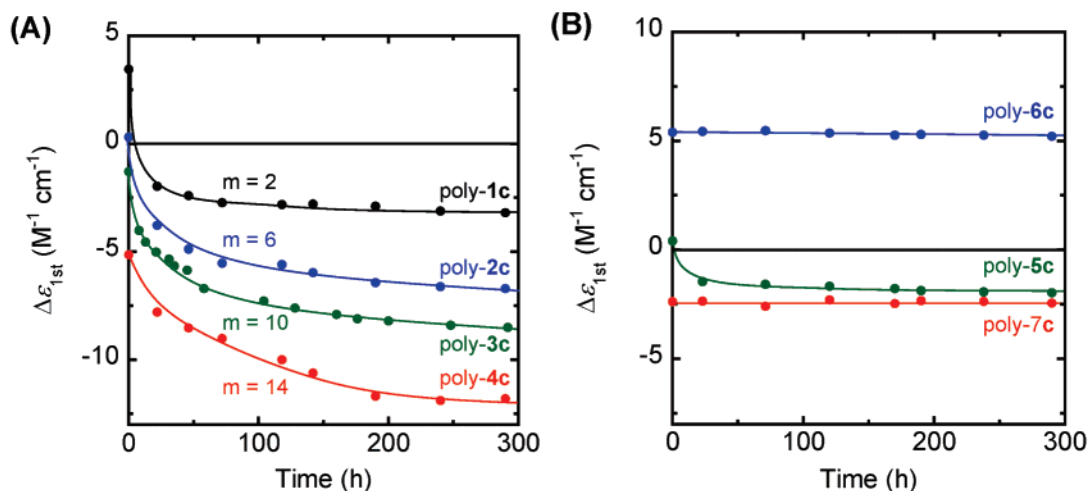


Figure 3. CD intensity changes of (A) poly-1c (black circles and line), poly-2c (blue circles and line), poly-3c (green circles and line), and poly-4c (red circles and line) and (B) poly-5c (green circles and line), poly-6c (blue circles and line), and poly-7c (red circles and line) with time in dilute toluene solution (0.2 mg/mL) at 100 °C.

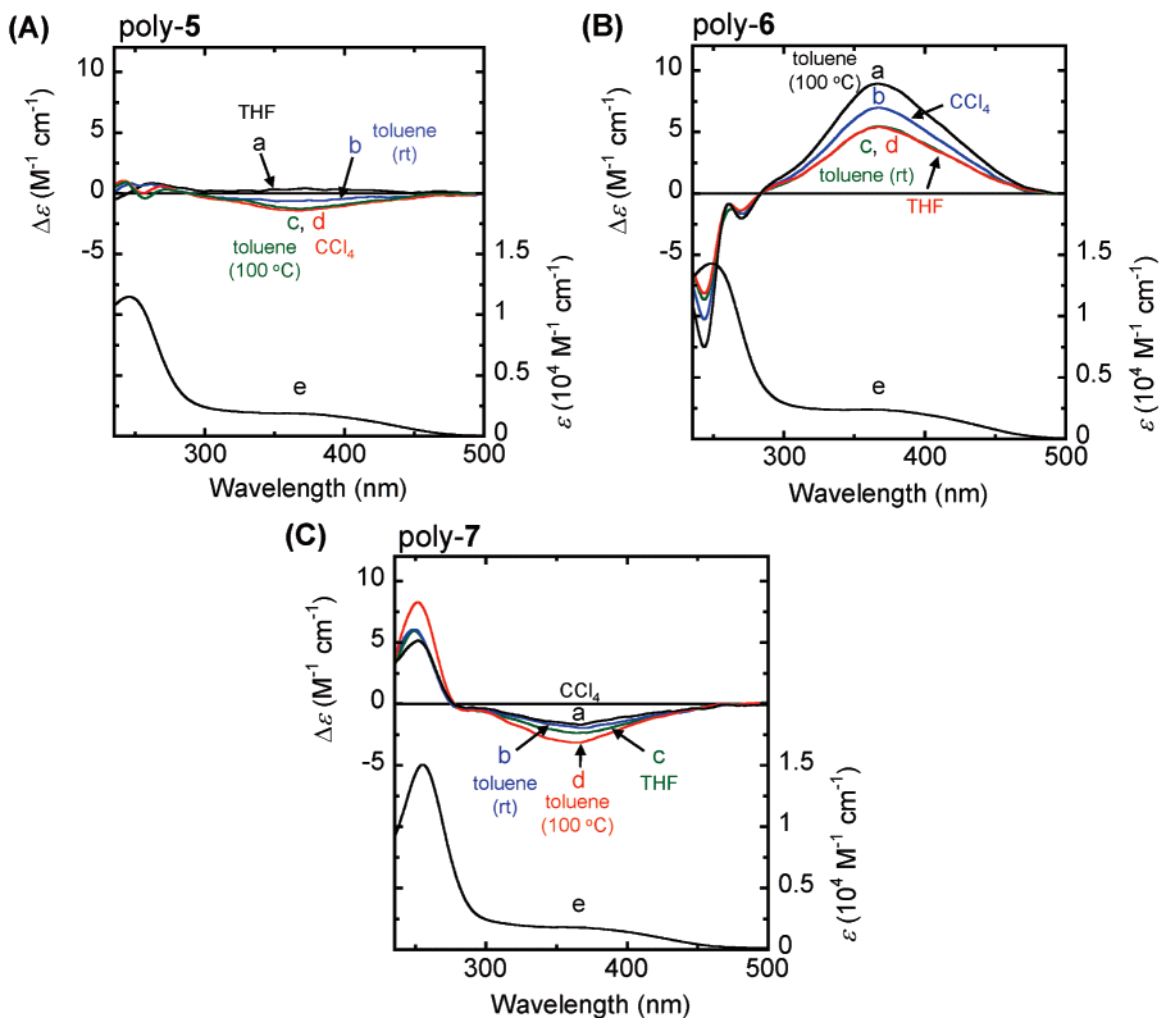


Figure 4. (A) CD spectra of poly-5c (a, black line), poly-5b (b, blue line), and poly-5a (d, red line) polymerized in THF, toluene, and CCl_4 , respectively, at room temperature, and poly-5d (c, green line) polymerized in toluene at 100 °C. The absorption spectrum of poly-5a (e) is also shown. (B) CD spectra of poly-6d (a, black line) polymerized in toluene at 100 °C, and poly-6a (b, blue line), poly-6b (c, green line), and poly-6c (d, red line) polymerized in CCl_4 , toluene, and THF, respectively, at room temperature. The absorption spectrum of poly-6a (e) is also shown. (C) CD spectra of poly-7a (a, black line), poly-7b (b, blue line), and poly-7c (c, green line) polymerized in CCl_4 , toluene, and THF, respectively, at room temperature, and poly-7d (d, red line) polymerized in toluene at 100 °C. The absorption spectrum of poly-7a (e) is also shown. The CD and absorption spectra were measured in $CHCl_3$ at 25 °C (0.2 mg/mL).

NH bands of poly-5s exceptionally shifted upward (3289–3301 cm^{-1}), and the ester carbonyl absorptions of poly-7s shifted to

longer wavenumbers (1748–1755 cm^{-1}). These results suggest that the amide NH groups of poly-1–poly-4 and poly-6 form

intramolecular hydrogen bonds not only with the amide carbonyl groups but also with the ester carbonyl groups in the neighboring pendants, which might play a crucial role in controlling the helical sense together with the excess one-handedness of polyisocyanides produced during the polymerization.

Consequently, the helical senses of polyisocyanides appear to be governed by a delicate balance of specific interactions (intermolecular hydrogen bonding and steric effect) occurring between the pendant residues of the growing chain end and monomers during the propagation reaction and can be controlled by the solvent polarity and temperature in the polymerization process and the pendant structures as well. This finding may be useful to design and synthesize new helical polyisocyanides with a controlled helical sense stable in solution, which will be further applicable to chiral materials for separating enantiomers as chiral stationary phases in chromatography.^{2,16}

Experimental Section

Instruments. NMR spectra were measured on a Varian AS500 spectrometer operating at 500 MHz for ¹H and 125 MHz for ¹³C, using TMS as the internal standard. IR spectra were recorded using a JASCO FT/IR-680 spectrometer. The absorption and CD spectra were obtained in a 1.0 mm quartz cell using a JASCO V570 spectrophotometer and a JASCO J820 spectropolarimeter, respectively. Temperature was controlled with JASCO ETC-505 and CDF-426 apparatuses for absorption and CD measurements, respectively. The polymer concentration was calculated on the basis of the monomer units and was 0.2 mg/mL. SEC was performed using a JASCO PU-2080 liquid chromatograph equipped with a UV-vis (JASCO UV-2070) and RI (JASCO RI-2031) detector. Two Tosoh TSKgel Multipore H_{XL}-M GPC columns (30 cm) were connected in series, and THF containing 0.1 wt % tetra-*n*-butylammonium bromide was used as the eluent at a flow rate of 0.8 mL/min. The molecular weight calibration curve was obtained with standard polystyrenes (Tosoh).

Materials. Anhydrous toluene, THF, CCl₄, CH₂Cl₂, CHCl₃, benzene, ethyl acetate, and ethanol (water content <50 ppm) were purchased from Wako (Osaka, Japan). Nickel(II) chloride hexahydrate (NiCl₂·6H₂O) and palladium 10% activated carbon were obtained from Aldrich. 4-Nitrobenzoic acid, *N,N'*-dicyclohexylcarbodiimide (DCC), 1-hydroxybenzotriazole monohydrate (HOBt), *N,N'*-dimethylacetamide (DMA), formic acid, acetic anhydride, triphosgene, and triethylamine were purchased from Wako, Tokyo Kasei (TCI, Tokyo, Japan), or Aldrich. These reagents were used without further purification.

Monomers **3** and **7**, poly-**3** (poly-**3a**–poly-**3d**), and poly-**7** (poly-**7a**–poly-**7d**) were prepared according to the previously reported methods.¹⁰ New optically active isocyanides (**1**, **2**, **4**–**6**) were prepared in the similar way as outlined in Scheme 2. The polymerization was performed with NiCl₂·6H₂O as the catalyst in different solvents at different temperatures (Scheme 1).

A Typical Procedure for Syntheses of 8, 9, and 11–13. HOBt (3.49 g, 22.8 mmol) and DCC (4.70 g, 22.8 mmol) were added to a solution of 4-nitrobenzoic acid (3.81 g, 22.8 mmol) in dry DMA (60 mL). After the reaction mixture was stirred at 0 °C for 30 min under Ar, the L-alanine ethyl ester (3.50 g, 22.8 mmol), which had been prepared from L-alanine and ethanol by the conventional method,¹¹ was added to the mixture. The dispersion solution was stirred at room temperature for 15 h and then at 120 °C for 5 h. After filtration, the solvent was removed under reduced pressure. The crude product was purified by silica gel chromatography with CHCl₃ as the eluent and then recrystallized with hexane–ethyl acetate (1:3, v/v) to give **8** as a white crystalline solid (4.13 g, 68%); mp 155.6–156.4 °C. IR (KBr, cm⁻¹): 3326 ($\nu_{\text{N-H}}$), 1692 ($\nu_{\text{C=O}}$ ester), 1626 (amide I), 1541 (amide II). ¹H NMR (CDCl₃, rt, 500 MHz): δ 1.33 (t, *J* = 7.0 Hz, CH₃, 3H), 1.56 (d, *J* = 7.0 Hz, CH₃, 3H), 4.24–4.30 (m, CH₂, 2H), 4.76–4.81 (m, CH, 1H), 6.92 (d, *J* = 7.5 Hz, NH, 1H), 7.98 (d, *J* = 9.0 Hz, aromatic, 2H), 8.30 (d, *J* = 9.0 Hz, aromatic, 2H). ¹³C NMR (CDCl₃, rt, 125

MHz): δ 14.15, 18.58, 49.43, 61.97, 123.85, 128.30, 139.55, 150.43, 164.78, 172.96. **9** and **11–13** were also prepared in the same way in 58, 80, 68, and 60% yield, respectively.

Spectroscopic data for **9**; mp 86.2–86.7 °C. IR (KBr, cm⁻¹): 3293 ($\nu_{\text{N-H}}$), 1739 ($\nu_{\text{C=O}}$ ester), 1639 (amide I), 1544 (amide II). ¹H NMR (CDCl₃, rt, 500 MHz): δ 0.90 (t, *J* = 7.0 Hz, CH₃, 3H), 1.28–1.41 (m, CH₂, 6H), 1.55 (d, *J* = 7.0 Hz, CH₃, 3H), 1.65–1.71 (m, CH₂, 2H), 4.16–4.24 (m, CH₂, 2H), 4.76–4.82 (m, CH, 1H), 6.97 (d, *J* = 7.5 Hz, NH, 1H), 7.97 (d, *J* = 9.0 Hz, aromatic, 2H), 8.30 (d, *J* = 9.0 Hz, aromatic, 2H). ¹³C NMR (CDCl₃, rt, 125 MHz): δ 14.21, 18.80, 22.74, 25.68, 28.69, 31.57, 49.11, 66.32, 124.05, 128.52, 139.71, 149.94, 164.97, 173.29.

Spectroscopic data for **11**; mp 91.4–92.0 °C. IR (KBr, cm⁻¹): 3297 ($\nu_{\text{N-H}}$), 1741 ($\nu_{\text{C=O}}$ ester), 1638 (amide I), 1527 (amide II). ¹H NMR (CDCl₃, rt, 500 MHz): δ 0.88 (t, *J* = 7.0 Hz, CH₃, 3H), 1.24–1.38 (m, CH₂, 22H), 1.55 (d, *J* = 7.0 Hz, CH₃, 3H), 1.65–1.71 (m, CH₂, 2H), 4.15–4.37 (m, CH₂, 2H), 4.75–4.81 (m, CH, 1H), 6.94 (d, *J* = 7.5 Hz, NH, 1H), 7.98 (d, *J* = 9.0 Hz, aromatic, 2H), 8.29 (d, *J* = 9.0 Hz, aromatic, 2H). ¹³C NMR (CDCl₃, rt, 125 MHz): δ 14.34, 18.82, 22.91, 25.97, 28.74, 29.41, 29.57, 29.71, 29.78, 29.86, 29.87, 29.88, 29.91, 32.14, 49.12, 66.30, 124.05, 128.51, 139.78, 149.97, 164.95, 173.23.

Spectroscopic data for **12**; mp 97.2–98.0 °C. IR (KBr, cm⁻¹): 3287 ($\nu_{\text{N-H}}$), 1638 (amide I), 1523 (amide II). ¹H NMR (CDCl₃, rt, 500 MHz): δ 0.88 (t, *J* = 7.0 Hz, CH₃, 3H), 1.22–1.38 (m, CH₃ and CH₂, 17H), 1.55–1.61 (m, CH₂, 2H), 3.44–3.48 (m, CH₂, 2H), 3.49–3.57 (m, CH₂, 2H), 4.34–4.39 (m, CH, 1H), 6.58 (d, *J* = 7.5 Hz, NH, 1H), 7.93 (d, *J* = 8.0 Hz, aromatic, 2H), 8.28 (d, *J* = 8.0 Hz, aromatic, 2H). ¹³C NMR (CDCl₃, rt, 125 MHz): δ 14.32, 17.99, 22.89, 26.41, 29.54, 29.67, 29.78, 29.81, 29.87, 32.11, 46.13, 71.75, 73.32, 123.97, 128.36, 140.68, 149.74, 164.98.

Spectroscopic data for **13**. Clear oil. IR (neat, cm⁻¹): 3294 ($\nu_{\text{N-H}}$), 1742 ($\nu_{\text{C=O}}$ ester), 1636 (amide I), 1527 (amide II). ¹H NMR (CDCl₃, rt, 500 MHz): δ 0.88 (t, *J* = 7.0 Hz, CH₃, 3H), 1.22–1.36 (m, CH₂, 14H), 1.56–1.68 (m, CH₂, 2H), 3.20–3.26 (m, CH₂, 2H), 4.12–4.17 (m, CH₂, 2H), 5.00–5.05 (m, CH, 1H), 6.32 (d, *J* = 7.0 Hz, NH, 1H), 7.21–7.33 (m, aromatic, 5H), 7.94 (d, *J* = 8.0 Hz, aromatic, 2H), 8.25 (d, *J* = 8.0 Hz, aromatic, 2H). ¹³C NMR (CDCl₃, rt, 125 MHz): δ 14.13, 21.60, 22.67, 25.84, 28.47, 29.20, 29.31, 29.52, 35.18, 38.07, 54.08, 65.91, 123.66, 127.18, 128.51, 128.61, 129.28, 136.08, 139.66, 150.69, 165.13, 171.55.

A Typical Procedure for Syntheses of 15, 16, and 18–20. Palladium-activated carbon (0.10 g) was added to a solution of **8** (0.70 g, 2.63 mmol) in ethanol (10 mL) and THF (10 mL). The mixture was stirred at room temperature for 7 h under an atmosphere of H₂. After filtrating using celite, the solvent was removed under reduced pressure. The crude product was then purified by recrystallization with hexane–ethyl acetate (1:3, v/v) to give **15** as a white crystalline solid (0.60 g, 97%); mp 164.6–165.1 °C. IR (KBr, cm⁻¹): 3445 ($\nu_{\text{N-H}}$), 3340 ($\nu_{\text{N-H}}$), 1736 ($\nu_{\text{C=O}}$ ester), 1630 (amide I), 1531 (amide II). ¹H NMR (CDCl₃, rt, 500 MHz): δ 1.32 (t, *J* = 7.0 Hz, CH₃, 3H), 1.50 (d, *J* = 7.0 Hz, CH₃, 3H), 3.97 (s, NH₂, 2H), 4.13–4.19 (m, CH₂, 2H), 4.74–4.80 (m, CH, 1H), 6.61 (d, *J* = 7.0 Hz, NH, 1H), 6.66 (d, *J* = 8.5 Hz, aromatic, 2H), 7.64 (d, *J* = 8.5 Hz, aromatic, 2H). ¹³C NMR (CDCl₃, rt, 125 MHz): δ 14.20, 18.63, 49.20, 62.41, 114.30, 123.80, 129.09, 149.93, 166.70, 173.70. **16** and **18–20** were also prepared in the same way in 89, 94, 91, and 85% yield, respectively.

Spectroscopic data for **16**; mp 142.4–143.6 °C. IR (KBr, cm⁻¹): 3445 ($\nu_{\text{N-H}}$), 3330 ($\nu_{\text{N-H}}$), 1739 ($\nu_{\text{C=O}}$ ester), 1630 (amide I), 1531 (amide II). ¹H NMR (CDCl₃, rt, 500 MHz): δ 0.89 (t, *J* = 7.0 Hz, CH₃, 3H), 1.28–1.38 (m, CH₂, 6H), 1.50 (d, *J* = 7.0 Hz, CH₃, 3H), 1.63–1.69 (m, CH₂, 2H), 4.00 (s, NH₂, 2H), 4.13–4.21 (m, CH₂, 2H), 4.74–4.80 (m, CH, 1H), 6.60 (d, *J* = 7.0 Hz, NH, 1H), 6.66 (d, *J* = 8.5 Hz, aromatic, 2H), 7.64 (d, *J* = 8.5 Hz, aromatic, 2H). ¹³C NMR (CDCl₃, rt, 125 MHz): δ 14.19, 19.16, 22.72, 25.69, 28.71, 31.58, 48.65, 65.89, 114.41, 123.86, 129.07, 149.87, 166.71, 173.87.

Spectroscopic data for **18**; mp 125.1–125.7 °C. IR (KBr, cm⁻¹): 3449 ($\nu_{\text{N-H}}$), 3344 ($\nu_{\text{N-H}}$), 1736 ($\nu_{\text{C=O}}$ ester), 1631 (amide I), 1531 (amide II). ¹H NMR (CDCl₃, rt, 500 MHz): δ 0.88 (t, *J* = 7.0 Hz,

CH₃, 3H), 1.23–1.39 (m, CH₂, 22H), 1.50 (d, $J = 7.0$ Hz, CH₃, 3H), 1.63–1.71 (m, CH₂, 2H), 3.98 (s, NH₂, 2H), 4.12–4.19 (m, CH₂, 2H), 4.74–4.80 (m, CH, 1H), 6.60 (d, $J = 7.0$ Hz, NH, 1H), 6.66 (d, $J = 8.5$ Hz, aromatic, 2H), 7.64 (d, $J = 8.5$ Hz, aromatic, 2H). ¹³C NMR (CDCl₃, rt, 125 MHz): δ 14.12, 18.96, 22.69, 25.82, 28.54, 29.21, 29.36, 29.56, 29.60, 29.64, 29.65, 29.67, 29.69, 31.93, 48.42, 65.67, 114.11, 123.58, 128.84, 149.75, 166.47, 173.64.

Spectroscopic data for **19**; mp 57.6–58.0 °C. IR (KBr, cm⁻¹): 3400 ($\nu_{\text{N-H}}$), 3289 ($\nu_{\text{N-H}}$), 1624 (amide I), 1536 (amide II). ¹H NMR (CDCl₃, rt, 500 MHz): δ 0.88 (t, $J = 7.0$ Hz, CH₃, 3H), 1.24–1.36 (m, CH₃ and CH₂, 17H), 1.54–1.60 (m, CH₂, 2H), 3.44–3.48 (m, CH₂, 2H), 3.49–3.52 (m, CH₂, 2H), 4.18 (s, NH₂, 2H), 4.31–4.34 (m, CH, 1H), 6.27 (d, $J = 7.5$ Hz, NH, 1H), 6.65 (d, $J = 8.0$ Hz, aromatic, 2H), 7.60 (d, $J = 8.0$ Hz, aromatic, 2H). ¹³C NMR (CDCl₃, rt, 125 MHz): δ 14.12, 17.99, 22.69, 26.20, 29.34, 29.48, 29.57, 29.62, 29.64, 31.90, 45.14, 71.42, 73.59, 114.13, 124.46, 128.63, 149.61, 166.54.

Spectroscopic data for **20**; mp 111.3–112.0 °C. IR (KBr, cm⁻¹): 3446 ($\nu_{\text{N-H}}$), 3327 ($\nu_{\text{N-H}}$), 1729 ($\nu_{\text{C=O}}$ ester), 1631 (amide I), 1532 (amide II). ¹H NMR (CDCl₃, rt, 500 MHz): δ 0.88 (t, $J = 7.0$ Hz, CH₃, 3H), 1.23–1.33 (m, CH₂, 14H), 1.57–1.62 (m, CH₂, 2H), 3.19–3.24 (m, CH₂, 2H), 3.48 (s, NH₂, 2H), 4.08–4.16 (m, CH₂, 2H), 5.02–5.07 (m, CH, 1H), 6.58 (d, $J = 7.5$ Hz, NH, 1H), 6.71 (d, $J = 8.5$ Hz, aromatic, 2H), 7.20–7.31 (m, aromatic, 5H), 7.57 (d, $J = 8.5$ Hz, aromatic, 2H). ¹³C NMR (CDCl₃, rt, 125 MHz): δ 14.13, 21.60, 22.68, 25.85, 28.46, 29.21, 29.30, 29.53, 35.23, 38.08, 53.50, 65.72, 114.92, 127.08, 128.53, 128.83, 129.42, 135.90, 136.11, 148.54, 166.53, 170.80.

A Typical Procedure for Syntheses of 22, 23, and 25–27. After a mixture of formic acid (0.479 mL, 12.7 mmol) and acetic anhydride (0.240 mL, 2.54 mmol) was stirred at room temperature for 1 h under Ar, **15** (0.60 g, 2.54 mmol) in dry ethyl acetate (20 mL) was added to the mixture at 0 °C. The dispersion was stirred at 0 °C for 30 min and then at room temperature for 30 min. To the solution was added ethyl acetate (50 mL), and the mixture was filtered. The filtrate was washed with H₂O (100 mL) and brine (100 mL) and then dried over anhydrous MgSO₄. After the solvent was removed under reduced pressure, the crude product was purified by SEC with CHCl₃ as the eluent and then recrystallized with hexane–ethyl acetate (1:3, v/v) to give **22** as a white crystalline solid (0.497 g, 74%); mp 142.9–143.7 °C. IR (KBr, cm⁻¹): 3358 ($\nu_{\text{N-H}}$), 3307 ($\nu_{\text{N-H}}$), 1737 ($\nu_{\text{C=O}}$ ester), 1634 (amide I), 1534 (amide II). ¹H NMR (CDCl₃, rt, 500 MHz): δ 1.33 (t, $J = 7.0$ Hz, CH₃, 3H), 1.54 (d, $J = 7.0$ Hz, CH₃, 3H), 4.24–4.28 (m, CH₂, 2H), 4.75–4.81 (m, CH, 1H), 6.74 (d, $J = 7.5$ Hz, NH, 1H), 7.14 (d, $J = 7.0$ Hz, H_o to NH in trans, 0.7H), 7.65 (d, $J = 7.0$ Hz, H_o to NH in cis, 1.3H), 7.81 (d, $J = 7.0$ Hz, H_m to NH in cis, 1.3H), 7.81 (d, $J = 7.0$ Hz, H_m to NH in trans, 0.7H), 8.44 (s, HCO, 1H), 8.82 (d, $J = 11.5$ Hz, NH, 1H). ¹³C NMR (CDCl₃, rt, 125 MHz): δ 14.16, 18.73, 48.61, 61.69, 117.70, 119.37, 128.28, 128.99, 139.89, 158.81, 161.39, 165.92, 173.29. **23** and **25–27** were also prepared in the same way in 73, 70, 54, and 48% yield, respectively.

Spectroscopic data for **23**; mp 134.5–134.9 °C. IR (KBr, cm⁻¹): 3355 ($\nu_{\text{N-H}}$), 3251 ($\nu_{\text{N-H}}$), 1747 ($\nu_{\text{C=O}}$ ester), 1635 (amide I), 1536 (amide II). ¹H NMR (CDCl₃, rt, 500 MHz): δ 0.89 (t, $J = 7.0$ Hz, CH₃, 3H), 1.27–1.41 (m, CH₂, 6H), 1.53 (d, $J = 7.0$ Hz, CH₃, 3H), 1.63–1.70 (m, CH₂, 2H), 4.13–4.22 (m, CH₂, 2H), 4.73–4.79 (m, CH, 1H), 6.86 (d, $J = 7.0$ Hz, NH in trans, 0.35H), 6.88 (d, $J = 7.0$ Hz, NH in cis, 0.65H), 7.12 (d, $J = 8.5$ Hz, H_o to NH in trans, 0.7H), 7.62 (d, $J = 8.5$ Hz, H_o to NH in cis, 1.3H), 7.76 (d, $J = 8.5$ Hz, H_m to NH in cis, 1.3H), 7.80 (d, $J = 8.5$ Hz, H_m to NH in trans, 0.7H), 8.09 (s, HCO in cis, 0.65H), 8.26 (d, $J = 9.5$ Hz, HCO in trans, 0.35H), 8.40 (d, $J = 2.0$ Hz, NH in cis, 0.65H), 8.80 (d, $J = 11.5$ Hz, NH in trans, 0.35H). ¹³C NMR (CDCl₃, rt, 125 MHz): δ 14.19, 18.81, 22.71, 25.68, 28.70, 31.56, 48.91, 66.04, 117.85, 119.64, 128.44, 129.17, 140.19, 140.43, 159.45, 162.05, 166.07, 166.46, 173.67.

Spectroscopic data for **25**; mp 129.5–130.1 °C. IR (KBr, cm⁻¹): 3355 ($\nu_{\text{N-H}}$), 3304 ($\nu_{\text{N-H}}$), 1742 ($\nu_{\text{C=O}}$ ester), 1639 (amide I), 1536 (amide II). ¹H NMR (CDCl₃, rt, 500 MHz): δ 0.88 (t, $J = 7.0$ Hz, CH₃, 3H), 1.23–1.38 (m, CH₂, 22H), 1.53 (d, $J = 7.5$ Hz, CH₃,

3H), 1.62–1.69 (m, CH₂, 2H), 4.15–4.21 (m, CH₂, 2H), 4.73–4.80 (m, CH, 1H), 6.70–6.78 (br, NH, 1H), 7.12 (d, $J = 9.0$ Hz, H_o to NH in trans, 0.7H), 7.55 (s, HCO in trans, 0.35H), 7.63 (d, $J = 9.0$ Hz, H_o to NH in cis, 1.3H), 7.79 (d, $J = 9.0$ Hz, H_m to NH in cis, 1.3H), 7.82 (d, $J = 9.0$ Hz, H_m to NH in trans, 0.7H), 7.89 (s, HCO in cis, 0.65H), 8.42 (d, $J = 1.5$ Hz, NH in cis, 0.65H), 8.80 (d, $J = 11.5$ Hz, NH in trans, 0.35H). ¹³C NMR (CDCl₃, rt, 125 MHz): δ 14.12, 18.77, 22.69, 25.81, 28.53, 29.20, 29.36, 29.50, 29.56, 29.64, 29.65, 29.67, 29.69, 31.92, 48.63, 65.86, 117.67, 119.37, 128.26, 128.98, 139.96, 140.24, 158.88, 161.58, 165.96, 166.17, 173.38.

Spectroscopic data for **26**; mp 120.0–120.8 °C. IR (KBr, cm⁻¹): 3309 ($\nu_{\text{N-H}}$), 1722 ($\nu_{\text{C=O}}$ ester), 1632 (amide I), 1541 (amide II). ¹H NMR (CDCl₃, rt, 500 MHz): δ 0.87 (t, $J = 7.0$ Hz, CH₃, 3H), 1.22–1.37 (m, CH₃ and CH₂, 17H), 1.56–1.59 (m, CH₂, 2H), 3.43–3.48 (m, CH₂, 2H), 3.49–3.55 (m, CH₂, 2H), 4.32–4.35 (m, CH, 1H), 6.48 (d, $J = 7.0$ Hz, NH, 1H), 7.13 (d, $J = 8.5$ Hz, H_o to NH in trans, 0.7H), 7.64 (d, $J = 8.5$ Hz, H_o to NH in cis, 1.3H), 7.72 (d, $J = 8.5$ Hz, H_m to NH in cis, 1.3H), 7.77 (d, $J = 8.5$ Hz, H_m to NH in trans, 0.7H), 8.39 (s, HCO, 1H), 8.80 (d, $J = 11.0$ Hz, NH, 1H). ¹³C NMR (CDCl₃, rt, 125 MHz): δ 14.32, 18.09, 22.88, 26.36, 29.52, 29.66, 29.78, 29.82, 29.87, 32.10, 45.76, 71.71, 73.56, 117.90, 119.65, 128.20, 128.96, 139.95, 140.34, 159.55, 162.11, 166.09, 166.50.

Spectroscopic data for **27**; mp 123.3–124.6 °C. IR (KBr, cm⁻¹): 3329 ($\nu_{\text{N-H}}$), 1733 ($\nu_{\text{C=O}}$ ester), 1634 (amide I), 1513 (amide II). ¹H NMR (CDCl₃, rt, 500 MHz): δ 0.88 (t, $J = 7.0$ Hz, CH₃, 3H), 1.22–1.34 (m, CH₂, 14H), 1.59–1.64 (m, CH₂, 2H), 3.22–3.29 (m, CH₂, 2H), 4.09–4.17 (m, CH₂, 2H), 5.04–5.08 (m, CH, 1H), 5.92 (d, $J = 7.0$ Hz, NH in trans, 0.5H), 6.54 (d, $J = 7.0$ Hz, NH in cis, 0.5H), 7.10 (d, $J = 8.0$ Hz, H_o to NH in trans, 1H), 7.13 (d, $J = 8.0$ Hz, H_o to NH in cis, 1H), 7.20–7.32 (m, aromatic, 5H), 7.61 (d, $J = 8.0$ Hz, H_m to NH in cis, 1H), 7.72 (d, $J = 8.0$ Hz, H_m to NH in trans, 1H), 8.42 (s, HCO, 1H), 8.79 (d, $J = 11.5$ Hz, NH, 1H). ¹³C NMR (CDCl₃, rt, 125 MHz): δ 14.39, 22.95, 23.48, 26.12, 28.71, 29.46, 29.57, 29.79, 32.15, 38.24, 53.40, 66.00, 119.65, 127.36, 128.50, 128.86, 129.64, 136.13, 140.18, 159.08, 165.88, 169.80, 172.02.

A Typical Procedure for Syntheses of 1, 2, and 4–6. Triethylamine (0.792 mL, 5.68 mmol) was added to a solution of **22** (750 mg, 2.84 mmol) in dry CH₂Cl₂ (10 mL). After the reaction mixture was stirred at 0 °C for 10 min under Ar, a solution of triphosgene (463 mg, 1.56 mmol) in CH₂Cl₂ (5 mL) was added dropwise to the mixture using a syringe. The dispersion was stirred at room temperature for 1 h, and then CH₂Cl₂ (50 mL) was added. After filtration, the solution was washed with aqueous NaHCO₃ (100 mL) and dried over anhydrous MgSO₄. The solvent was removed under reduced pressure, and the crude product was purified by silica gel chromatography with CHCl₃ as the eluent and then recrystallized with hexane–ethyl acetate (1:1, v/v) to give **1** as a white crystalline solid (510 mg, 73%); mp 80.4–80.9 °C. IR (KBr, cm⁻¹): 3294 ($\nu_{\text{N-H}}$), 2129 ($\nu_{\text{C}\equiv\text{N}}$), 1740 ($\nu_{\text{C=O}}$ ester), 1638 (amide I), 1542 (amide II). ¹H NMR (CDCl₃, rt, 500 MHz): δ 1.30 (t, $J = 7.0$ Hz, CH₃, 3H), 1.54 (d, $J = 7.0$ Hz, CH₃, 3H), 4.20–4.26 (m, CH₂, 2H), 4.75–4.81 (m, CH, 1H), 6.76 (d, $J = 6.5$ Hz, NH, 1H), 7.40 (d, $J = 8.5$ Hz, aromatic, 2H), 7.81 (d, $J = 8.5$ Hz, aromatic, 2H). ¹³C NMR (CDCl₃, rt, 125 MHz): δ 14.16, 18.80, 49.12, 61.99, 126.62, 128.60, 129.14, 135.01, 164.84, 166.94, 173.01. Anal. Calcd (%) for C₁₃H₁₄N₂O₃ (246.3): C, 63.40; H, 5.73; N, 11.38. Found (%): C, 63.38; H, 5.55; N, 11.35. $[\alpha]_{\text{D}}^{25} +13.5$ (c 0.3, CHCl₃). **2** and **4–6** were also prepared in the same way in 66, 71, 46, and 58% yield, respectively.

Spectroscopic data for **2**; mp 82.0–82.6 °C. IR (KBr, cm⁻¹): 3294 ($\nu_{\text{N-H}}$), 2126 ($\nu_{\text{C}\equiv\text{N}}$), 1742 ($\nu_{\text{C=O}}$ ester), 1638 (amide I), 1542 (amide II). ¹H NMR (CDCl₃, rt, 500 MHz): δ 0.88 (t, $J = 7.0$ Hz, CH₃, 3H), 1.24–1.38 (m, CH₂, 6H), 1.52 (d, $J = 7.0$ Hz, CH₃, 3H), 1.62–1.70 (m, CH₂, 2H), 4.14–4.25 (m, CH₂, 2H), 4.73–4.80 (m, CH, 1H), 6.98 (d, $J = 7.0$ Hz, NH, 1H), 7.41 (d, $J = 8.5$ Hz, aromatic, 2H), 7.84 (d, $J = 8.5$ Hz, aromatic, 2H). ¹³C NMR (CDCl₃, rt, 125 MHz): δ 14.25, 18.83, 22.79, 26.04, 28.70, 32.12, 49.21, 66.20, 126.65, 128.69, 129.30, 134.97, 165.10, 167.07,

173.56. Anal. Calcd (%) for $C_{17}H_{22}N_2O_3$ (302.4): C, 67.53; H, 7.33; N, 9.26. Found (%): C, 67.50; H, 7.09; N, 9.07. $[\alpha]_D^{25} +14.6$ (c 0.3, $CHCl_3$).

Spectroscopic data for **4**; mp 103.2–103.6 °C. IR (KBr, cm^{-1}): 3294 (ν_{N-H}), 2129 ($\nu_{C\equiv N}$), 1740 ($\nu_{C=O}$ ester), 1638 (amide I), 1542 (amide II). 1H NMR ($CDCl_3$, rt, 500 MHz): δ 0.86 (t, $J = 7.0$ Hz, CH_3 , 3H), 1.24–1.35 (m, CH_2 , 22H), 1.50 (d, $J = 7.0$ Hz, CH_3 , 3H), 1.62–1.68 (m, CH_2 , 2H), 4.12–4.20 (m, CH_2 , 2H), 4.73–4.79 (m, CH, 1H), 6.95 (d, $J = 7.0$ Hz, NH, 1H), 7.45 (d, $J = 8.5$ Hz, aromatic, 2H), 7.76 (d, $J = 8.5$ Hz, aromatic, 2H). ^{13}C NMR ($CDCl_3$, rt, 125 MHz): δ 14.30, 18.87, 22.89, 26.03, 28.72, 29.31, 29.35, 29.52, 29.48, 29.54, 29.61, 29.64, 29.66, 32.03, 48.91, 65.97, 126.68, 128.63, 129.27, 135.07, 165.14, 166.91, 173.50. Anal. Calcd (%) for $C_{25}H_{38}N_2O_3$ (414.6): C, 72.43; H, 9.24; N, 6.76. Found (%): C, 72.26; H, 9.17; N, 6.77. $[\alpha]_D^{25} +12.2$ (c 0.3, $CHCl_3$).

Spectroscopic data for **5**; mp 92.3–92.7 °C. IR (KBr, cm^{-1}): 3298 (ν_{N-H}), 2130 ($\nu_{C\equiv N}$), 1632 (amide I), 1540 (amide II). 1H NMR ($CDCl_3$, rt, 500 MHz): δ 0.88 (t, $J = 7.0$ Hz, CH_3 , 3H), 1.24–1.35 (m, CH_3 and CH_2 , 17H), 1.58–1.63 (m, CH_2 , 2H), 3.41–3.46 (m, CH_2 , 2H), 3.47–3.53 (m, CH_2 , 2H), 4.30–4.38 (m, CH, 1H), 6.73 (d, $J = 7.0$ Hz, NH, 1H), 7.42 (d, $J = 8.5$ Hz, aromatic, 2H), 7.82 (d, $J = 8.5$ Hz, aromatic, 2H). ^{13}C NMR ($CDCl_3$, rt, 125 MHz): δ 14.27, 17.98, 22.90, 26.40, 29.25, 29.49, 29.75, 29.80, 29.84, 32.03, 45.81, 71.64, 73.62, 126.49, 128.60, 129.03, 135.24, 165.26, 167.01. Anal. Calcd (%) for $C_{21}H_{32}N_2O_2$ (344.5): C, 73.22; H, 9.36; N, 8.13. Found (%): C, 73.22; H, 9.40; N, 8.13. $[\alpha]_D^{25} -7.46$ (c 0.3, $CHCl_3$).

Spectroscopic data for **6**. Brown oil. IR (neat, cm^{-1}): 3294 (ν_{N-H}), 2129 ($\nu_{C\equiv N}$), 1738 ($\nu_{C=O}$ ester), 1630 (amide I), 1516 (amide II). 1H NMR ($CDCl_3$, rt, 500 MHz): δ 0.87 (t, $J = 7.0$ Hz, CH_3 , 3H), 1.24–1.35 (m, CH_2 , 14H), 1.58–1.63 (m, CH_2 , 2H), 3.20–3.31 (m, CH_2 , 2H), 4.11–4.19 (m, CH_2 , 2H), 4.98–5.07 (m, CH, 1H), 6.91 (d, $J = 7.0$ Hz, NH, 1H), 7.20–7.30 (m, aromatic, 5H), 7.37 (d, $J = 8.5$ Hz, aromatic, 2H), 7.75 (d, $J = 8.5$ Hz, aromatic, 2H). ^{13}C NMR ($CDCl_3$, rt, 125 MHz): δ 14.29, 23.01, 23.50, 26.10, 28.95, 29.51, 29.59, 29.77, 32.01, 38.20, 53.47, 66.18, 119.68, 127.30, 128.57, 128.86, 129.61, 136.01, 139.40, 140.14, 165.64, 169.81, 173.54. Anal. Calcd (%) for $C_{27}H_{34}N_2O_3$ (434.6): C, 74.62; H, 7.89; N, 6.45. Found (%): C, 74.60; H, 7.87; N, 6.28. $[\alpha]_D^{25} +43.1$ (c 0.3, $CHCl_3$).

Polymerization. Polymerization was carried out in a dry glass ampule under a dry N_2 atmosphere with $NiCl_2 \cdot 6H_2O$ as the catalyst in a way similar to that previously reported.^{9c,10} A typical polymerization procedure is described below. Monomer **1** (50 mg, 0.20 mmol) was placed in a dry ampule, which was then evacuated under a vacuum line and flushed with dry N_2 . After this evacuation–flush procedure was repeated three times, a three-way stopcock was attached to the ampule, and dry CCl_4 (2.0 mL) was added with a syringe. To this was added a solution of $NiCl_2 \cdot 6H_2O$ in dry ethanol (0.1 M, 0.02 mL) at room temperature. The concentrations of the monomer and the Ni catalyst were 0.1 and 0.001 M, respectively. After 1 day, the resulting polymer was precipitated into a large amount of methanol, collected by centrifugation, and then dried in vacuo at room temperature for 2 h to give poly-**1a** (45.1 mg, 90%). IR (KBr, cm^{-1}): 3278 (ν_{N-H}), 1740 ($\nu_{C=O}$ ester), 1637 (amide I), 1536 (amide II). 1H NMR ($CDCl_3$, rt, 500 MHz): δ 1.22 (broad, CH_3 , 3H), 1.53 (broad, CH_3 , 3H), 4.11 (broad, CH_2 , 2H), 4.46 (broad, CH, 1H), 4.8–7.9 (broad, aromatic, 4H), 8.1–9.0 (broad, NH, 1H). Anal. Calcd (%) for $(C_{13}H_{14}N_2O_3)_n$: C, 63.40; H, 5.73; N, 11.38. Found (%): C, 63.42; H, 5.62; N, 11.23. $[\alpha]_D^{25} +680$ (c 0.1, $CHCl_3$). In the same way, poly-**2a**, poly-**4a**, poly-**5a**, and poly-**6a** in CCl_4 at room temperature, poly-**1b**, poly-**2b**, poly-**4b**, poly-**5b**, and poly-**6b** in toluene at room temperature, poly-**1c**, poly-**2c**, poly-**4c**, poly-**5c**, and poly-**6c** in THF at room temperature, poly-**1d**, poly-**2d**, poly-**4d**, poly-**5d**, and poly-**6d** in toluene at 100 °C, poly-**3e** in toluene at 50 °C, poly-**3f** in toluene at 75 °C, poly-**3g** in benzene at room temperature, poly-**3h** in $CHCl_3$ at room temperature, and poly-**3i** in CH_2Cl_2 at room temperature were prepared in 83, 43, 72, 64, 80, 75, 65, 64, 70, 87, 80, 87, 87, 79, 72, 85, 77, 81, 80, 85, 78, 80, 88, and 92% yields, respectively.

Spectroscopic data for poly-**1b**. IR (KBr, cm^{-1}): 3271 (ν_{N-H}), 1741 ($\nu_{C=O}$ ester), 1637 (amide I), 1535 (amide II). 1H NMR ($CDCl_3$, rt, 500 MHz): δ 1.26 (broad, CH_3 , 3H), 1.52 (broad, CH_3 , 3H), 4.11 (broad, CH_2 , 2H), 4.43 (broad, CH, 1H), 4.9–7.9 (broad, aromatic, 4H), 8.1–8.9 (broad, NH, 1H). $[\alpha]_D^{25} +377$ (c 0.1, $CHCl_3$).

Spectroscopic data for poly-**1c**. IR (KBr, cm^{-1}): 3276 (ν_{N-H}), 1742 ($\nu_{C=O}$ ester), 1638 (amide I), 1534 (amide II). 1H NMR ($CDCl_3$, rt, 500 MHz): δ 1.25 (broad, CH_3 , 3H), 1.53 (broad, CH_3 , 3H), 4.12 (broad, CH_2 , 2H), 4.45 (broad, CH, 1H), 5.0–8.0 (broad, aromatic, 4H), 8.1–9.1 (broad, NH, 1H). $[\alpha]_D^{25} +247$ (c 0.1, $CHCl_3$).

Spectroscopic data for poly-**1d**. IR (KBr, cm^{-1}): 3282 (ν_{N-H}), 1744 ($\nu_{C=O}$ ester), 1636 (amide I), 1535 (amide II). 1H NMR ($CDCl_3$, rt, 500 MHz): δ 1.25 (broad, CH_3 , 3H), 1.52 (broad, CH_3 , 3H), 4.11 (broad, CH_2 , 2H), 4.43 (broad, CH, 1H), 4.8–7.8 (broad, aromatic, 4H), 8.1–9.0 (broad, NH, 1H). $[\alpha]_D^{25} -1180$ (c 0.1, $CHCl_3$).

Spectroscopic data for poly-**2a**. IR (KBr, cm^{-1}): 3266 (ν_{N-H}), 1741 ($\nu_{C=O}$ ester), 1637 (amide I), 1535 (amide II). 1H NMR ($CDCl_3$, rt, 500 MHz): δ 0.83 (broad, CH_3 , 3H), 1.26 (broad, CH_2 , 6H), 1.57 (broad, CH_3 and CH_2 , 5H), 4.05 (broad, CH_2 , 2H), 4.42 (broad, CH, 1H), 5.0–7.8 (broad, aromatic, 4H), 8.1–9.1 (broad, NH, 1H). Anal. Calcd (%) for $(C_{17}H_{22}N_2O_3)_n$: C, 67.53; H, 7.33; N, 9.26. Found (%): C, 67.55; H, 7.56; N, 9.18. $[\alpha]_D^{25} +1020$ (c 0.1, $CHCl_3$).

Spectroscopic data for poly-**2b**. IR (KBr, cm^{-1}): 3277 (ν_{N-H}), 1742 ($\nu_{C=O}$ ester), 1637 (amide I), 1535 (amide II). 1H NMR ($CDCl_3$, rt, 500 MHz): δ 0.83 (broad, CH_3 , 3H), 1.25 (broad, CH_2 , 6H), 1.54 (broad, CH_3 , 3H), 1.68 (broad, CH_2 , 2H), 4.04 (broad, CH_2 , 2H), 4.41 (broad, CH, 1H), 5.0–7.9 (broad, aromatic, 4H), 8.0–9.1 (broad, NH, 1H). $[\alpha]_D^{25} +146$ (c 0.1, $CHCl_3$).

Spectroscopic data for poly-**2c**. IR (KBr, cm^{-1}): 3281 (ν_{N-H}), 1742 ($\nu_{C=O}$ ester), 1637 (amide I), 1535 (amide II). 1H NMR ($CDCl_3$, rt, 500 MHz): δ 0.83 (broad, CH_3 , 3H), 1.25 (broad, CH_2 , 6H), 1.53 (broad, CH_3 , 3H), 1.61 (broad, CH_2 , 2H), 4.04 (broad, CH_2 , 2H), 4.41 (broad, CH, 1H), 5.0–7.8 (broad, aromatic, 4H), 8.0–9.0 (broad, NH, 1H). $[\alpha]_D^{25} +55.3$ (c 0.1, $CHCl_3$).

Spectroscopic data for poly-**2d**. IR (KBr, cm^{-1}): 3272 (ν_{N-H}), 1742 ($\nu_{C=O}$ ester), 1637 (amide I), 1535 (amide II). 1H NMR ($CDCl_3$, rt, 500 MHz): δ 0.83 (broad, CH_3 , 3H), 1.26 (broad, CH_2 , 6H), 1.55 (broad, CH_3 and CH_2 , 5H), 4.06 (broad, CH_2 , 2H), 4.48 (broad, CH, 1H), 5.0–7.9 (broad, aromatic, 4H), 8.1–9.0 (broad, NH, 1H). $[\alpha]_D^{25} -705$ (c 0.1, $CHCl_3$).

Spectroscopic data for poly-**3e**. IR (KBr, cm^{-1}): 3286 (ν_{N-H}), 1742 ($\nu_{C=O}$ ester), 1637 (amide I), 1534 (amide II). 1H NMR ($CDCl_3$, rt, 500 MHz): δ 0.88 (broad, CH_3 , 3H), 1.26 (broad, CH_2 , 14H), 1.56 (broad, CH_3 and CH_2 , 5H), 4.07 (broad, CH_2 , 2H), 4.47 (broad, CH, 1H), 5.0–7.9 (broad, aromatic, 4H), 8.1–9.1 (broad, NH, 1H). $[\alpha]_D^{25} +60.8$ (c 0.1, $CHCl_3$).

Spectroscopic data for poly-**3f**. IR (KBr, cm^{-1}): 3294 (ν_{N-H}), 1743 ($\nu_{C=O}$ ester), 1637 (amide I), 1534 (amide II). 1H NMR ($CDCl_3$, rt, 500 MHz): δ 0.87 (broad, CH_3 , 3H), 1.26 (broad, CH_2 , 14H), 1.55 (broad, CH_3 and CH_2 , 5H), 4.06 (broad, CH_2 , 2H), 4.46 (broad, CH, 1H), 5.0–7.8 (broad, aromatic, 4H), 8.1–9.0 (broad, NH, 1H). $[\alpha]_D^{25} -137$ (c 0.1, $CHCl_3$).

Spectroscopic data for poly-**3g**. IR (KBr, cm^{-1}): 3277 (ν_{N-H}), 1742 ($\nu_{C=O}$ ester), 1637 (amide I), 1534 (amide II). 1H NMR ($CDCl_3$, rt, 500 MHz): δ 0.87 (broad, CH_3 , 3H), 1.25 (broad, CH_2 , 14H), 1.55 (broad, CH_3 , 3H), 1.65 (broad, CH_2 , 2H), 4.04 (broad, CH_2 , 2H), 4.42 (broad, CH, 1H), 5.0–7.9 (broad, aromatic, 4H), 8.0–9.0 (broad, NH, 1H). $[\alpha]_D^{25} +325$ (c 0.1, $CHCl_3$).

Spectroscopic data for poly-**3h**. IR (KBr, cm^{-1}): 3274 (ν_{N-H}), 1743 ($\nu_{C=O}$ ester), 1636 (amide I), 1535 (amide II). 1H NMR ($CDCl_3$, rt, 500 MHz): δ 0.87 (broad, CH_3 , 3H), 1.26 (broad, CH_2 , 14H), 1.54 (broad, CH_3 , 3H), 1.64 (broad, CH_2 , 2H), 4.03 (broad, CH_2 , 2H), 4.41 (broad, CH, 1H), 5.0–7.8 (broad, aromatic, 4H), 8.0–9.0 (broad, NH, 1H). $[\alpha]_D^{25} +293$ (c 0.1, $CHCl_3$).

Spectroscopic data for poly-**3i**. IR (KBr, cm^{-1}): 3277 (ν_{N-H}), 1743 ($\nu_{C=O}$ ester), 1636 (amide I), 1534 (amide II). 1H NMR ($CDCl_3$, rt, 500 MHz): δ 0.87 (broad, CH_3 , 3H), 1.25 (broad, CH_2 ,

14H), 1.54 (broad, CH₃, 3H), 1.61 (broad, CH₂, 2H), 4.04 (broad, CH₂, 2H), 4.41 (broad, CH, 1H), 5.0–7.8 (broad, aromatic, 4H), 8.0–9.0 (broad, NH, 1H). [α]_D²⁵ +56.4 (c 0.1, CHCl₃).

Spectroscopic data for poly-**4a**. IR (KBr, cm⁻¹): 3268 (ν_{N-H}), 1743 ($\nu_{C=O}$ ester), 1636 (amide I), 1535 (amide II). ¹H NMR (CDCl₃, rt, 500 MHz): δ 0.88 (broad, CH₃, 3H), 1.26 (broad, CH₂, 22H), 1.54 (broad, CH₃, 3H), 1.60 (broad, CH₂, 2H), 4.04 (broad, CH₂, 2H), 4.43 (broad, CH, 1H), 5.0–7.9 (broad, aromatic, 4H), 8.0–9.0 (broad, NH, 1H). Anal. Calcd (%) for (C₂₅H₃₈N₂O₃)_n: C, 72.43; H, 9.24; N, 6.76. Found (%): C, 72.43; H, 9.24; N, 6.66. [α]_D²⁵ +671 (c 0.1, CHCl₃).

Spectroscopic data for poly-**4b**. IR (KBr, cm⁻¹): 3277 (ν_{N-H}), 1743 ($\nu_{C=O}$ ester), 1636 (amide I), 1534 (amide II). ¹H NMR (CDCl₃, rt, 500 MHz): δ 0.88 (broad, CH₃, 3H), 1.26 (broad, CH₂, 22H), 1.57 (broad, CH₃ and CH₂, 5H), 4.04 (broad, CH₂, 2H), 4.44 (broad, CH, 1H), 5.0–7.9 (broad, aromatic, 4H), 8.1–9.1 (broad, NH, 1H). [α]_D²⁵ +155 (c 0.1, CHCl₃).

Spectroscopic data for poly-**4c**. IR (KBr, cm⁻¹): 3293 (ν_{N-H}), 1743 ($\nu_{C=O}$ ester), 1637 (amide I), 1534 (amide II). ¹H NMR (CDCl₃, rt, 500 MHz): δ 0.88 (broad, CH₃, 3H), 1.26 (broad, CH₂, 22H), 1.55 (broad, CH₃, 3H), 1.68 (broad, CH₂, 2H), 4.05 (broad, CH₂, 2H), 4.44 (broad, CH, 1H), 5.0–7.8 (broad, aromatic, 4H), 8.0–9.0 (broad, NH, 1H). [α]_D²⁵ -326 (c 0.1, CHCl₃).

Spectroscopic data for poly-**4d**. IR (KBr, cm⁻¹): 3282 (ν_{N-H}), 1744 ($\nu_{C=O}$ ester), 1636 (amide I), 1535 (amide II). ¹H NMR (CDCl₃, rt, 500 MHz): δ 0.88 (broad, CH₃, 3H), 1.26 (broad, CH₂, 22H), 1.60 (broad, CH₃ and CH₂, 5H), 4.04 (broad, CH₂, 2H), 4.42 (broad, CH, 1H), 5.0–7.9 (broad, aromatic, 4H), 8.1–9.1 (broad, NH, 1H). [α]_D²⁵ -420 (c 0.1, CHCl₃).

Spectroscopic data for poly-**5a**. IR (KBr, cm⁻¹): 3297 (ν_{N-H}), 1631 (amide I), 1536 (amide II). ¹H NMR (CDCl₃, rt, 500 MHz): δ 0.87 (broad, CH₃, 3H), 1.26 (broad, CH₂, 14H), 1.54 (broad, CH₃, 3H), 1.69 (broad, CH₂, 2H), 3.44 (broad, CH₂, 4H), 4.41 (broad, CH, 1H), 4.9–7.9 (broad, aromatic, 4H), 8.0–8.9 (broad, NH, 1H). Anal. Calcd (%) for (C₂₁H₃₂N₂O₂)_n: C, 73.22; H, 9.36; N, 8.13. Found (%): C, 73.23; H, 9.45; N, 7.99. [α]_D²⁵ -177 (c 0.1, CHCl₃).

Spectroscopic data for poly-**5b**. IR (KBr, cm⁻¹): 3301 (ν_{N-H}), 1636 (amide I), 1541 (amide II). ¹H NMR (CDCl₃, rt, 500 MHz): δ 0.87 (broad, CH₃, 3H), 1.26 (broad, CH₂, 14H), 1.53 (broad, CH₃, 3H), 1.58 (broad, CH₂, 2H), 3.42 (broad, CH₂, 4H), 4.20 (broad, CH, 1H), 4.7–7.8 (broad, aromatic, 4H), 7.9–8.9 (broad, NH, 1H). [α]_D²⁵ -107 (c 0.1, CHCl₃).

Spectroscopic data for poly-**5c**. IR (KBr, cm⁻¹): 3297 (ν_{N-H}), 1636 (amide I), 1535 (amide II). ¹H NMR (CDCl₃, rt, 500 MHz): δ 0.86 (broad, CH₃, 3H), 1.25 (broad, CH₂, 14H), 1.50 (broad, CH₃ and CH₂, 5H), 3.42 (broad, CH₂, 4H), 4.20 (broad, CH, 1H), 4.8–7.8 (broad, aromatic, 4H), 8.0–8.9 (broad, NH, 1H). [α]_D²⁵ -64.2 (c 0.1, CHCl₃).

Spectroscopic data for poly-**5d**. IR (KBr, cm⁻¹): 3290 (ν_{N-H}), 1632 (amide I), 1535 (amide II). ¹H NMR (CDCl₃, rt, 500 MHz): δ 0.86 (broad, CH₃, 3H), 1.26 (broad, CH₂, 14H), 1.50 (broad, CH₃, 3H), 1.77 (broad, CH₂, 2H), 3.42 (broad, CH₂, 4H), 4.22 (broad, CH, 1H), 4.9–7.9 (broad, aromatic, 4H), 8.0–8.9 (broad, NH, 1H). [α]_D²⁵ -273 (c 0.1, CHCl₃).

Spectroscopic data for poly-**6a**. IR (KBr, cm⁻¹): 3276 (ν_{N-H}), 1742 ($\nu_{C=O}$ ester), 1637 (amide I), 1534 (amide II). ¹H NMR (CDCl₃, rt, 500 MHz): δ 0.88 (broad, CH₃, 3H), 1.26 (broad, CH₂, 14H), 1.56 (broad, CH₂, 2H), 3.32 (broad, CH₂, 2H), 3.96 (broad, CH₂, 2H), 4.94 (broad, CH, 1H), 5.2–8.0 (broad, aromatic, 9H), 8.4–9.3 (broad, NH, 1H). Anal. Calcd (%) for (C₂₇H₃₄N₂O₃)_n: C, 74.62; H, 7.89; N, 6.45. Found (%): C, 74.63; H, 7.97; N, 6.40. [α]_D²⁵ +439 (c 0.1, CHCl₃).

Spectroscopic data for poly-**6b**. IR (KBr, cm⁻¹): 3276 (ν_{N-H}), 1743 ($\nu_{C=O}$ ester), 1637 (amide I), 1534 (amide II). ¹H NMR (CDCl₃, rt, 500 MHz): δ 0.87 (broad, CH₃, 3H), 1.26 (broad, CH₂, 14H), 1.60 (broad, CH₂, 2H), 3.32 (broad, CH₂, 2H), 3.95 (broad, CH₂, 2H), 4.94 (broad, CH, 1H), 5.2–8.3 (broad, aromatic, 9H), 8.4–9.3 (broad, NH, 1H). [α]_D²⁵ +390 (c 0.1, CHCl₃).

Spectroscopic data for poly-**6c**. IR (KBr, cm⁻¹): 3278 (ν_{N-H}), 1743 ($\nu_{C=O}$ ester), 1638 (amide I), 1534 (amide II). ¹H NMR (CDCl₃, rt, 500 MHz): δ 0.87 (broad, CH₃, 3H), 1.26 (broad, CH₂,

14H), 1.57 (broad, CH₂, 2H), 3.34 (broad, CH₂, 2H), 3.96 (broad, CH₂, 2H), 4.94 (broad, CH, 1H), 5.2–8.0 (broad, aromatic, 9H), 8.4–9.4 (broad, NH, 1H). [α]_D²⁵ +364 (c 0.1, CHCl₃).

Spectroscopic data for poly-**6d**. IR (KBr, cm⁻¹): 3275 (ν_{N-H}), 1743 ($\nu_{C=O}$ ester), 1637 (amide I), 1534 (amide II). ¹H NMR (CDCl₃, rt, 500 MHz): δ 0.88 (broad, CH₃, 3H), 1.26 (broad, CH₂, 14H), 1.56 (broad, CH₂, 2H), 3.33 (broad, CH₂, 2H), 3.96 (broad, CH₂, 2H), 4.93 (broad, CH, 1H), 5.2–7.6 (broad, aromatic, 9H), 8.2–9.3 (broad, NH, 1H). [α]_D²⁵ +688 (c 0.1, CHCl₃).

Supporting Information Available: FT-IR data of poly-**1**–poly-**7**, ¹H NMR and IR spectra of **3** in various solvents, plots of the $\Delta\epsilon_{\text{1st}}$ values of poly-**3b**, poly-**3c**, poly-**3g**, and poly-**3i** vs the chemical shift of the amide proton resonances of **3** and the amide II band of **3** in various solvents, plots of molar rotation vs molar ellipticity at the first Cotton effect of poly-**1**–poly-**7**, CD and absorption spectra of poly-**1**–poly-**4**, and CD intensity changes of poly-**3a** and poly-**3d** with time in toluene at 100 °C. This information is available free of charge via the Internet at <http://pubs.acs.org>.

References and Notes

- (1) For examples, see: (a) Yu, S. M.; Conticello, V. P.; Zhang, G.; Kayser, C.; Fourinier, M. J.; Mason, T. L.; Tirrell, D. A. *Nature (London)* **1997**, *389*, 167–170. (b) Green, M. M.; Zanella, S.; Gu, H.; Sato, T.; Gottarelli, G.; Jha, S. K.; Spada, G. P.; Schoevaars, A. M.; Feringa, B.; Teramoto, A. *J. Am. Chem. Soc.* **1998**, *120*, 9810–9817. (c) Watanabe, J.; Kamee, H.; Fujiki, M. *Polym. J.* **2001**, *33*, 495–497. (d) Cornelissen, J. J. L. M.; Donners, J. J. J. M.; de Gelder, R.; Graswinckel, W. S.; Metselaar, G. A.; Rowan, A. E.; Sommerdijk, N. A. J. M.; Nolte, R. J. M. *Science* **2001**, *293*, 676–680. (e) Cornelissen, J. J. L. M.; Graswinckel, W. S.; Rowan, A. E.; Sommerdijk, N. A. J. M.; Nolte, R. J. M. *J. Polym. Sci., Part A: Polym. Chem.* **2003**, *41*, 1725–1736. (f) Kim, J.; Novak, B. M. *Macromolecules* **2004**, *37*, 1660–1662. (g) Tian, G.; Lu, Y.; Novak, B. M. *J. Am. Chem. Soc.* **2004**, *126*, 4082–4083. (h) Maeda, K.; Takeyama, Y.; Sakajiri, K.; Yashima, E. *J. Am. Chem. Soc.* **2004**, *126*, 16284–16285. (i) Okoshi, K.; Sakajiri, K.; Kumaki, J.; Yashima, E. *Macromolecules* **2005**, *38*, 4061–4064. (j) Metselaar, G. A.; Wezenberg, S. J.; Cornelissen, J. J. L. M.; Nolte, R. J. M.; Rowan, A. E. *J. Polym. Sci., Part A: Polym. Chem.* **2007**, *45*, 981–988.
- (2) (a) Okamoto, Y.; Yashima, E. *Angew. Chem., Int. Ed.* **1998**, *37*, 1021–1043. (b) Yashima, E. *J. Chromatogr. A* **2001**, *906*, 105–125. (c) Nakano, T. *J. Chromatogr. A* **2001**, *906*, 205–225. (d) Nakano, T.; Okamoto, Y. *Chem. Rev.* **2001**, *101*, 4013–4038. (e) Yamamoto, C.; Okamoto, Y. *Bull. Chem. Soc. Jpn.* **2004**, *77*, 227–257.
- (3) For reviews on helical polymers, see ref 2d and: (a) Green, M. M.; Park, J.-W.; Sato, T.; Teramoto, A.; Lifson, S.; Selinger, R. L. B.; Selinger, J. V. *Angew. Chem., Int. Ed.* **1999**, *38*, 3138–3154. (b) Cornelissen, J. J. L. M.; Rowan, A. E.; Nolte, R. J. M.; Sommerdijk, N. J. A. M. *Chem. Rev.* **2001**, *101*, 4039–4070. (c) Fujiki, M. *Macromol. Rapid Commun.* **2001**, *22*, 539–563. (d) Nomura, R.; Nakano, H.; Masuda, T. *J. Mol. Catal. A* **2002**, *190*, 197–205. (e) Yashima, E.; Maeda, K.; Nishimura, T. *Chem.—Eur. J.* **2004**, *10*, 43–51. (f) Lam, J. W. Y.; Tang, B. Z. *Acc. Chem. Res.* **2005**, *38*, 745–754.
- (4) For reviews on helical polyisocyanides, see ref 3b and: (a) Millich, F. *Chem. Rev.* **1972**, *72*, 101–113. (b) Millich, F. *Adv. Polym. Sci.* **1975**, *19*, 117–141. (c) Drenth, W.; Nolte, R. J. M. *Acc. Chem. Res.* **1979**, *12*, 30–35. (d) Nolte, R. J. M. *Chem. Soc. Rev.* **1994**, *23*, 11–19. (e) Takahashi, S.; Onitsuka, K.; Takei, F. *Proc. Jpn. Acad.* **1998**, *74(B)*, 25–30. (f) Sugimoto, M.; Ito, Y. *Adv. Polym. Sci.* **2004**, *171*, 77–136. (g) Amabilino, D. B.; Serrano, J.-L.; Sierra, T.; Veciana, J. *J. Polym. Sci., Part A: Polym. Chem.* **2006**, *44*, 3161–3174. For other leading references on helical polyisocyanides, see: (h) Kamer, P. C. J.; Cleij, M. C.; Nolte, R. J. M.; Harada, T.; Hezemans, A. M. F.; Drenth, W. *J. Am. Chem. Soc.* **1988**, *110*, 1581–1587. (i) Green, M. M.; Gross, R. A.; Schilling, F. C.; Zero, K.; Crosby, C. I. *Macromolecules* **1988**, *21*, 1839–1846. (j) Pini, D.; Iuliano, A.; Salvadori, P. *Macromolecules* **1992**, *25*, 6059–6062. (k) Takei, F.; Yanai, K.; Onitsuka, K.; Takahashi, S. *Angew. Chem., Int. Ed.* **1996**, *35*, 1554–1556. (l) Spencer, L.; Kim, M.; Euler, W. B.; Rosen, W. *J. Am. Chem. Soc.* **1997**, *119*, 8129–8130. (m) Cornelissen, J. J. L. M.; Fischer, M.; Sommerdijk, N. A. J. M.; Nolte, R. J. M. *Science* **1998**, *280*, 1427–1430. (n) Amabilino, D. B.; Ramos, E.; Serrano, J.-L.; Veciana, J. *Adv. Mater.* **1998**, *10*, 1001–1005. (o) Amabilino, D. B.; Ramos, E.; Serrano, J.-L.; Sierra, T.; Veciana, J. *J. Am. Chem. Soc.* **1998**, *120*, 9126–9134. (p) Hasegawa, T.; Kondoh, S.; Matsuura, K.; Kobayashi, K. *Macromolecules* **1999**, *32*,

- 6595–6603. (q) Takei, F.; Yanai, K.; Onitsuka, K.; Takahashi, S. *Chem.—Eur. J.* **2000**, *6*, 983–993. (r) Yamada, Y.; Kawai, T.; Abe, J.; Iyoda, T. *J. Polym. Sci., Part A: Polym. Chem.* **2002**, *40*, 399–408. (s) Metselaar, G. A.; Cornelissen, J. J. L. M.; Rowan, A. E.; Nolte, R. J. M. *Angew. Chem., Int. Ed.* **2005**, *44*, 1990–1993. (t) Amabilino, D. B.; Ramos, E.; Serrano, J.-L.; Sierra, T.; Veciana, J. *Polymer* **2005**, *46*, 1507–1521. (u) Onitsuka, K.; Mori, T.; Yamamoto, M.; Takei, F.; Takahashi, S. *Macromolecules* **2006**, *39*, 7224–7231.
- (5) (a) van Beijnen, A. J. M.; Nolte, R. J. M.; Drenth, W.; Hezemans, A. M. F. *Tetrahedron* **1976**, *32*, 2017–2019. (b) van Beijnen, A. J. M.; Nolte, R. J. M.; Naaktgebornen, A. J.; Zwikker, J. W.; Drenth, W.; Hezemans, A. M. F. *Macromolecules* **1983**, *16*, 1679–1689. (c) Takei, F.; Hayashi, H.; Onitsuka, K.; Kobayashi, N.; Takahashi, S. *Angew. Chem., Int. Ed.* **2001**, *40*, 4092–4094. (d) Cornelissen, J. J. L. M.; Sommerdijk, N. A. J. M.; Nolte, R. J. M. *Macromol. Chem. Phys.* **2002**, *203*, 1625–1630. Recently, the helical structure of an optically active polyisocyanide was determined to be a 15 units/4 turns (15/4) helix with a helical pitch of 1.28 nm on the basis of X-ray diffraction combined with high-resolution atomic force microscopy (AFM) observations. See: (e) Onouchi, H.; Okoshi, K.; Kajitani, T.; Sakurai, S.-i.; Nagai, K.; Onitsuka, K.; Yashima, E. *J. Am. Chem. Soc.* **2008**, *130*, 229–236.
- (6) Nolte, R. J. M.; van Beijnen, A. J. M.; Drenth, W. *J. Am. Chem. Soc.* **1974**, *96*, 5932–5933.
- (7) Kamer, P. C. J.; Nolte, R. J. M.; Drenth, W. *J. Am. Chem. Soc.* **1988**, *110*, 6818–6825.
- (8) Deming, T. J.; Novak, B. M. *J. Am. Chem. Soc.* **1992**, *114*, 7926–7927.
- (9) (a) Kauranen, K.; Verbiest, T.; Boutton, C.; Teerenstra, M. N.; Schouten, A. J.; Nolte, R. J. M.; Persoons, A. *Science* **1995**, *270*, 966–969. (b) Cornelissen, J. J. L. M.; Graswinckel, W. S.; Adams, P. J. H. M.; Nachtegaal, G. H.; Kentgens, A. P. M.; Sommerdijk, N. A. J. M.; Nolte, R. J. M. *J. Polym. Sci., Part A: Polym. Chem.* **2001**, *39*, 4255–4264. (c) Ishikawa, M.; Maeda, K.; Yashima, E. *J. Am. Chem. Soc.* **2002**, *124*, 7448–7458. (d) Gomar-Nadal, E.; Veciana, J.; Rovira, C.; Amabilino, D. B. *Adv. Mater.* **2005**, *17*, 2095–2098. (e) Kros, A.; Jesse, W.; Metselaar, G. A.; Cornelissen, J. J. L. M. *Angew. Chem., Int. Ed.* **2005**, *44*, 4349–4352. (f) Tian, Y.; Kamata, K.; Yoshida, H.; Iyoda, T. *Chem.—Eur. J.* **2006**, *12*, 584–591. (g) Hase, Y.; Mitsutsuji, Y.; Ishikawa, M.; Maeda, K.; Okoshi, K.; Yashima, E. *Chem. Asian J.* **2007**, *2*, 755–763.
- (10) Kajitani, T.; Okoshi, K.; Sakurai, S.-i.; Kumaki, J.; Yashima, E. *J. Am. Chem. Soc.* **2006**, *128*, 708–709.
- (11) Because the right- and left-handed helices of poly-**3s** are diastereomers, therefore, their CD spectra, in particular in the pendant aromatic regions (235–280 nm), differ from one another. In addition, high-resolution AFM observations of the diastereomeric poly-**3s** revealed that the polyisocyanides showing a positive $\Delta\epsilon_{1st}$ value have a right-handed helical structure.^{5e,10}
- (12) For the hydrogen-bond-assisted helical polymers except for poly-(isocyanopeptides)s, see: (a) Nomura, R.; Tabei, J.; Masuda, T. *J. Am. Chem. Soc.* **2001**, *123*, 8430–8431. (b) Li, B. S.; Cheuk, K. K. L.; Ling, L.; Chen, J.; Xiao, X.; Bai, C.; Tang, B. Z. *Macromolecules* **2003**, *36*, 77–85.
- (13) Reichardt, C. In *Solvents and Solvent Effects in Organic Chemistry*, 3rd ed.; Wiley-VCH: Weinheim, 2003; pp 375–388.
- (14) A similar increase in the CD intensity upon heating was recently reported for the poly(aryl isocyanide)s with chiral pendants. See: (a) Takei, F.; Onitsuka, K.; Takahashi, S. *Macromolecules* **2005**, *38*, 1513–1516. For other reversible and irreversible changes in the CD spectral patterns by temperature or reduction-oxidation cycles, see: (b) Hida, N.; Takei, F.; Onitsuka, K.; Shiga, K.; Asaoka, S.; Iyoda, T.; Takahashi, S. *Angew. Chem., Int. Ed.* **2003**, *42*, 4349–4352. (c) Amabilino, D. B.; Serrano, J.-L.; Veciana, J. *Chem. Commun.* **2005**, 322–324. (d) Wezenberg, S. J.; Metselaar, G. A.; Rowan, A. E.; Cornelissen, J. J. L. M.; Seebach, D.; Nolte, R. J. M. *Chem.—Eur. J.* **2006**, *12*, 2778–2786. (e) Metselaar, G. A.; Adams, P. J. H. M.; Nolte, R. J. M.; Cornelissen, J. J. L. M.; Rowan, A. E. *Chem.—Eur. J.* **2007**, *13*, 950–960.
- (15) Poly-**3a** also showed a slight decrease in its $\Delta\epsilon_{1st}$ value of ca. 5 % after annealing in a mixture of toluene and dimethylformamide (DMF) (3:2, v/v) at 100 °C for 445 h.
- (16) (a) Yamagishi, A.; Tanaka, I.; Taniguchi, M.; Takahashi, M. *J. Chem. Soc., Chem. Commun.* **1994**, 1113–1114. (b) Tsuchida, A.; Hasegawa, T.; Kobayashi, K.; Yamamoto, C.; Okamoto, Y. *Bull. Chem. Soc. Jpn.* **2002**, *75*, 2681–2685.

MA7022952